

AD-A254 969



2

Ocean Optical Database

S **DTIC**
ELECTE
AUG 26 1992 **D**
A

R. A. Arnone
Remote Sensing Branch
Ocean Sensing and Prediction Division
Ocean Science Directorate

G. Terrie
L. Estep
Mapping, Charting, and Geodesy Division
Ocean Science Directorate

R. A. Oriol
Planning Systems Incorporated
Slidell, LA 70458

✓
*Original contains color
plates: All DTIC reproductions
will be in black and
white*



Approved for public release; distribution is unlimited. Naval Oceanographic and Atmospheric Research Laboratory, Stennis Space Center, Mississippi 39529-5004.

92-23642

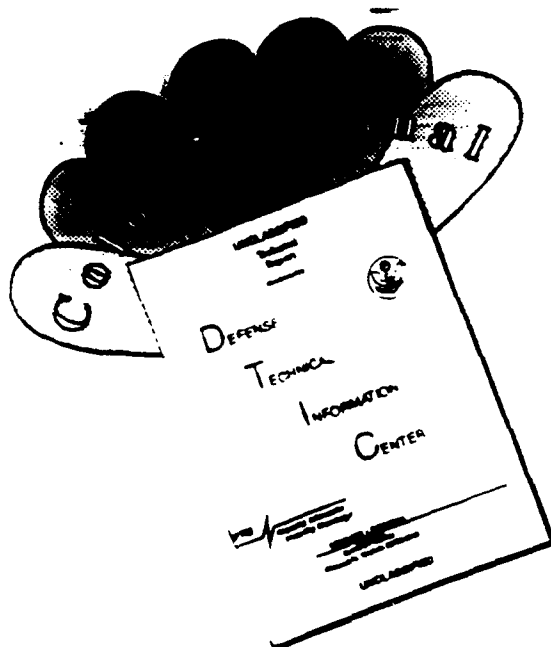


92 8 25 976

42148.5

4/2/92

DISCLAIMER NOTICE



THIS DOCUMENT IS BEST QUALITY AVAILABLE. THE COPY FURNISHED TO DTIC CONTAINED A SIGNIFICANT NUMBER OF COLOR PAGES WHICH DO NOT REPRODUCE LEGIBLY ON BLACK AND WHITE MICROFICHE.

Abstract

The global ocean optical property of the diffuse attenuation coefficient at 490 nm $k(490)$, has been assembled into a database using satellite ocean color data from the Coastal Zone Color Scanner. The database representing 6 years of satellite coverage from 1978 to 1986 is at a spatial resolution of 20 km and is represented in monthly composites. The assemblage and format of the data are defined.

Problems and limitations of using satellite ocean color for retrieving ocean $k(490)$ values are examined. The validation of the optical database from the satellite is accessed through comparison with in situ ship measurements of chlorophyll and diffuse attenuation coefficient.

Accession For	
NTIS CRA&I	<input checked="" type="checkbox"/>
DTIC TAB	<input type="checkbox"/>
Unannounced	<input type="checkbox"/>
Justification	
By	
Distribution/	
Availability Codes	
Dist	Avail and/or Special
A-1	

Acknowledgments

This effort was supported by the Oceanographer of the Navy, OP-096, (under the program Coastal Optics Planner) (PE 0603741N) and SPAWARS, Air Defense Initiative (PE 0603785N) ASW program. Special thanks is extended to these program managers, K. Ferer and G. Morris for their confidence and foresight in establishing advanced applications of satellite data. Without their financial support, these efforts could not have been performed. Appreciation is extended to C. McClain and G. Fu of the NASA/Goddard Space Flight Center for their support and responsiveness with SeaPak software. Appreciation is extended to W. Esaias and B. Balch for sharing results of this validation study. We wish to thank J. Mueller for helpful discussions in optics and satellite processing and for sharing his ships satellite data. Additionally, gratitude is extended to A. Weidemann and K. Davis for their help with supporting optical data. Credit is extended to Bigelow Laboratories for supplying k(490) data. Recognition is extended to the JPL for supplying the NASA Ocean Data System sea surface temperature data.

The mention of commercial products or the use of company names does not in any way imply endorsement by the U.S. Navy or NOARL.

Ocean Optical Database

Introduction

The oceans' optical environment has recently been shown to be much more variable than previously believed (Yoder et al., 1987; Lewis et al., 1988). Historically, ocean optical properties have been an extremely laborious task to measure. Ship optical measurements were and still are extremely time consuming and costly. Additionally, ocean optical properties are affected by the apparent light field such as solar radiation, altitude, azimuth, and other environmental conditions such as wave height. All these problems coupled with the effects of ship shadow (Voss et al., 1986) have limited the availability of high quality ocean properties and therefore have restricted our understanding of the spatial and temporal variability of ocean optical properties.

Recent efforts within the past 10 years have focused on exploiting the use of ocean color or spectral water leaving radiance as a method of addressing the spatial and temporal variability of ocean optical properties (Austin and Petzold, 1984; Mueller et al., 1990). Ocean color satellite data has distinct advantages of rapidly collecting imagery in global oceans and can illustrate the spatial changing ocean optical properties associated with different water masses. Additionally, imagery can be collected in daily increments so that the temporal changes can be easily observed. The changing optical properties are readily observed from one day to the next as a response of the biological conditions in the surface ocean. Recent results have shown that in dynamic ocean regions such as the Alboran Sea in the Mediterranean Sea, the chlorophyll concentrations decreased to one-half its concentration within a 24-h period (Arnone and La Violette, 1991). Additionally through the effort of examining the total ocean color satellite data set, a picture of the global distribution of the bio-optical environment has been acquired. This new look on the changing bio-optical character of the oceans has served to enrich our understanding of dynamic biological and optical processes.

Objective

The objective of this paper is to characterize the global optical variability of surface ocean water through a database acquired by Coastal Zone Color Scanner (CZCS) satellite data. The methods of constructing monthly climatology of the diffuse attenuation coefficient or $k(490)$ are described. The database has specific application in defining the spatial and temporal scales of optical variability. The format of the optical database is described in addition to methods of accessing the available products. This database of global optical climatology represents a valuable tool for assessing Navy system performance of electro-optical systems in the ocean. With the planned launch of new

ocean color satellite, SeaWiFS, this database provides an initial understanding of long term changes in ocean optical structure.

CZCS Ocean Color

CZCS was the first spaceborne sensor designed specifically to measure subtle changes in ocean color. CZCS had six coregistered bands (five visible and one in the thermal infrared, IR) with a swath and resolution (2200 km and 825 m at nadir, respectively). CZCS collected approximately 66,000 2-min scenes of high spectral resolution ocean color data from November 1978 to June 1986. The CZCS provided absolute radiance distribution in four spectral regions to discriminate biological and geological differences in water masses and were centered at 443, 520, and 550 (Hovis et al., 1980; Gordon et al., 1983). Because the atmospheric scattering contributed approximately 80 to 90% of the total radiance sensed by the spaceborne sensor, processing techniques to eliminate the atmosphere are required (Gordon, 1978; Gordon and Clark, 1981). Atmospheric correction required utilizing the 670-nm channel on CZCS to estimate the aerosol path radiance and subtraction of Rayleigh and aerosol scattering from the three visible channels (Gordon and Clark, 1980a, 1981; Gordon, 1978). Thus, the absolute spectral "water leaving radiance" ocean color is obtained for each pixel in CZCS imagery. To eliminate the effect of the solar elevation on the CZCS derived radiance, the radiance were normalized to a 90° solar zenith (Gordon et al., 1983).

Level 1 CZCS data represents data that has not been atmospherically corrected. Following processing to remove atmospheric noise and to derive absolute water leaving radiance, the CZCS data is elevated to level 2. Level-3 data represents geometric registration of the level-2 data to a map projection.

The derived products generated by the CZCS level-2 programs are water radiance at 443, 520, and 550 nm, and aerosol radiance at 670 nm. The absolute spectral radiance has been shown to be empirically correlated with the optical property of the diffuse attenuation coefficient at 490 nm by Austin and Petzold, 1984. The diffuse attenuation coefficient, $k(490)$ is the rate of decay of light in ocean waters at 490 nm. High (turbid) $k(490)$ values, which are characterized in coastal waters, have values above 0.2 m^{-1} , whereas the oligotrophic (clear) waters of the Sargasso Sea have values of 0.04 m^{-1} . This empirical relationship was formulated from ship measurements as the ratio of the radiance at 443:550 nm and $k(490)$. This relationship was shown to have a correlation coefficient (r^2) of 0.98. A similar relationship of the ratio of 443:550 spectral water leaving radiance was found for the chlorophyll pigments concentration (Gordon and Clark, 1980a; Clark, 1981). The k algorithm as it is presently known, was expanded by Mueller et al., 1990, to coastal (Case 2) waters by using the ratio of the 520:550 spectral radiance in k waters greater then 0.16. (The 443 radiance approaches 0 in high chlorophyll coastal regions and 443:550 algorithm is not useable.) These relationships are shown as:

$$(1) \quad k(490) = 0.0883 \left(\text{Lu}443 / \text{Lu}550 \right)^{-1.491} + 0.022$$

$$r^2 = 0.901$$

if $k(490) > 0.16$ then

$$(2) \quad k(490) = 0.17728 \left(\text{Lu}520 / \text{Lu}550 \right)^{-2.914} + 0.022$$

where Lu = water leaving radiance at 443 nm.

Additionally, methods to discriminate ocean regions, which are optically shallow and are contaminated by bottom reflectance, have been incorporated into improved processing of CZCS radiance (Arnone et al., 1990). These improvements to the k algorithm are known as the k-branch algorithm. This algorithm was based on ship measurements and has been extended into CZCS spectral water leaving radiance. Thus, the CZCS data can be used to derive the diffuse attenuation coefficient at 490 nm (K490).

The diffuse attenuation coefficient at 490 nm can be converted to the k at another wavelength through the algorithm developed by Austin and Petzold, 1984. This equation takes the form:

$$(3) \quad K_{\lambda 2} = [M_{\lambda 2} / M_{\lambda 1}] \{ K_{\lambda 1} - K_{\lambda 2} \} + K_{w \lambda 2}$$

where $M_{\lambda 1}$ is the coefficient for wavelength 2. The conversion relationship of k to multiwavelength has been found to hold across the visible spectrum.

Limitation and Assumptions of Optical Properties Derived from Ocean Color

There are problems associated with using ocean color data for estimating the ocean optical properties. Understanding these limitations is required to appreciate the optical database that has been established. Foremost of these problems is that ocean color satellite data represents only surface properties. Spectral radiance distributions sensed at the surface is an integrated value through the first attenuation length (Gordon and McCluney, 1975), and therefore, the optical properties that are derived from the color signature represent only the near surface. (The first attenuation length is the depth that the surface radiance decays to 1 logarithm of the surface value; typically, the Gulf Stream is approximately 20 m and Slope water is 8-10 m.)

The vertical distribution of the optical properties can vary significantly from the surface signature (Cullen and Eppley, 1981; Mueller and Lange, 1989; Platt et al., 1991). The optical properties have been shown to change substantially at the mixed-layer depth

(Kitchen and Zaneveld, 1990). In certain conditions, the change in density occurring at the mixed-layer depth results in high nutrient concentrations occurring in the lower interface waters. The biological activity of increased chlorophyll growth results in development of a "chlorophyll maximum." These high concentrations represent turbid water conditions occurring at or near the mixed-layer depth. Because the mixed-layer depth can be below the first attenuation length, the satellite derived optical properties are **NOT** representing the total vertical optical properties. In review of these satellite optical data, the variability of the vertical profile of $k(490)$ should be considered in interpretation of the satellite products. Presently, efforts are being developed to model this vertical distribution (Platt et al., 1991; Mueller and Lange, 1989).

The ocean optical properties have been separated into Case 1 and Case 2 waters (Morel and Prieur, 1977). In deep ocean waters (Case 1), the optical properties covary with the chlorophyll concentrations. Absorption of chlorophyll controls the optical distribution. In coastal waters (Case 2), the optical properties are influenced by biogenics (suspended sediments, dissolved organics etc.) in addition to chlorophyll concentrations. The variability of coastal waters (Case 2) is more complex and difficult to model since scattering of the particles controls the optical distribution.

Satellite derived optical properties require absolute measurements of the water leaving radiance in each of the spectral channels. Quantitative ocean color measurements from space require several items be properly monitored and known through the life of the satellite. Errors in these items have a cascading error in the accurate quantitative water leaving radiance and therefore the absolute $k(490)$ values obtained. The items are listed in importance:

1. CZCS on-board sensor calibration and drift of the sensitivity of the detectors.

With CZCS the detectors were observed to decay with time from the launch of the satellite. The blue channel had decayed the most in June of 1986 where the response was 40% of the launch sensitivity. The decay coefficients of the channel sensitivity is programmed into CZCS processing; however, there is error in this estimate. (Evans, personnel communication).

2. Atmospheric correction procedures have inherent errors.

- a. The 670-nm channel, which is assumed representative of the aerosol optical depth, is not correct in coastal sediment laden waters or in areas of high coccolithophores (Mueller, 1984; Smith and Wilson, 1981; Arnone, 1983). As the waters become more concentrated with sediment, the 670 radiance increases and the assumptions of the atmospheric algorithm departs from an estimate of aerosol scattering. The resulting spectral water leaving radiance can be shown to be overestimated as the radiance at 670 nm increases from sediment concentration

increases. This tends to overestimate the $k(490)$ values.

b. The aerosol type (size, shape, composition, etc.) is assumed uniform both spatially and temporally in CZCS processing. The Angstrom coefficient (η) (Gordon et al., 1980a, 1983) was selected as 0 representing a continental air mass for all CZCS processing. (The Angstrom coefficient represents the optical aerosol depth dependence on wavelength. This parameter changes with different types of aerosols). Assuming a uniform (η) induces an error since the aerosol type changes both spatially and temporally within the global CZCS data set. By not selecting the coefficient for each individual image, the optimum aerosol depth was not selected. Although this allowed for rapid computer processing, the error in resulting $k(490)$ can be considerable for certain ocean regions where the aerosol type departs from a continental air mass. Of course the composite imagery has been averaged over a 1-month period, which would blend the errors resulting from variability of aerosol character.

Global CZCS Products

The establishment of a global optical property database was constructed based on historical CZCS data. Goddard Space Flight Center (GSFC) processed the 66,000 scenes of CZCS data into specific products (Feldman, 1989; Esaias et al., 1986). A climatology of the CZCS spectral radiance distribution has been compiled for the world ocean at a reduced 20-km² resolution and averaged over a 1-month period (Feldman et al., 1989). CZCS had a ground resolution of approximately 1 km and repeat time of approximately 4 times a week. The high resolution CZCS imagery were averaged over a 20-km cell and over monthly time periods to produce a climatology of the mean and standard deviation. The monthly climatology has been created for 92 months for the life of the CZCS satellite (November 1978 - June 1986).

The CZCS digital data available from Goddard used to construct the database were the 20 x 20 km PST "postage-stamp" image file format of the University of Miami's Rosenthal School of Marine and Atmospheric Sciences (RSMAS)/DSP image analysis system. This file format is used in the global CZCS processing activity (Feldman et al., 1989). The image represented by the PST file is an equirectangular image of the world (90° N to 90° S and 180° W to 180° E) containing 2048 x 1024 pixels. Each of these pixels is referred to as a "bin" representing approximately 20 x 20 km at the equator. Each bin contains data from the corresponding pixels of the higher resolution image(s) used to generate the PST file. Goddard processing of the PST image format assumed a standard atmosphere applied to all the scenes to increase the rate at which the scenes could be processed (Feldman et al., 1989).

Global PST files have been reformatted and compiled into an optical database by the Ocean Color Laboratory using the PC-SeaPak image processing system (Firestone

et al., 1989; McClain et al., 1990). This optical database is intended for use with the PC-SeaPak image processing software package to provide statistical manipulation of the data products. PC-SeaPak is an interactive satellite data analysis package that is being developed at NASA/(GSFC) Ocean Processes Branch and is designed to operate on an IBM PC-AT class microcomputer. It is a subset of the SeaPak analysis system (McClain et al., 1990) that runs on a DEC VAX-based system at the Oceans Computing Facility at GSFC.

The optical database segments the globe into eight regions (**Figure 1**). (Four in the Northern Hemisphere and four in the Southern Hemisphere). This organization of the database was selected to cover the prime oceanic areas in each hemisphere. The optical database at a 20-km spatial resolution is composed of the following products:

1. Mean 443 normalized radiance ($\mu\text{W}/\text{cm}^2/\text{nm}$)
2. Standard Deviation at 443 normalized radiance ($\mu\text{W}/\text{cm}^2/\text{nm}$)
3. Mean 520 normalized radiance ($\mu\text{W}/\text{cm}^2/\text{nm}$)
4. Standard Deviation at 520 normalized radiance ($\mu\text{W}/\text{cm}^2/\text{nm}$)
5. Mean 550 normalized radiance ($\mu\text{W}/\text{cm}^2/\text{nm}$)
6. Standard Deviation 550 normalized radiance ($\mu\text{W}/\text{cm}^2/\text{nm}$)
7. Mean 670 aerosol radiance ($\mu\text{W}/\text{cm}^2/\text{nm}$)
8. Standard Deviation 670 aerosol radiance ($\mu\text{W}/\text{cm}^2/\text{nm}$)
9. Mean Chlorophyll Concentration (Gordon and Clark's algorithm) mg/m^3
10. Standard deviation Chlorophyll Concentration mg/m^3
11. Mean Diffuse attenuation Coefficient $k(490)$ Austin and Petzold's algorithm
12. Standard Deviation $k(490)$
13. Number of scenes (dates) used in making each 20-km pixel
14. Number of pixels used in the 20-km average

Each of these data products are displayable as 512 x 512 8-bit image maps compatible with the PC-SeaPak image format. Valid data ranges are from 1 to 255 (gray levels), which are transformed into absolute geophysical units. A header file written into each product permits the PC-SeaPak software to navigate and derive the desired geophysical parameters.

An example of mean and standard deviation for radiance distribution for Region 2 (North Atlantic) is illustrated in **Figure 2** for April 1979. Similarly, the examples of $k(490)$, and chlorophyll and the number of pixels used in the composite and number of scenes used in the composite are shown in **Figure 3** for the same area. Land areas and areas of no data are assigned 0 values. Areas of no data may exist due to the following:

- High scan angle of the sensor
- Cloud cover and/or aerosol contamination
- Sensor not activated over offshore oceanic regions



Figure 1. The satellite global optical database is segmented into eight regions shown here. This example represents the mean monthly $k(490)$ for April 1979. The large black areas represent locations where no data is available.

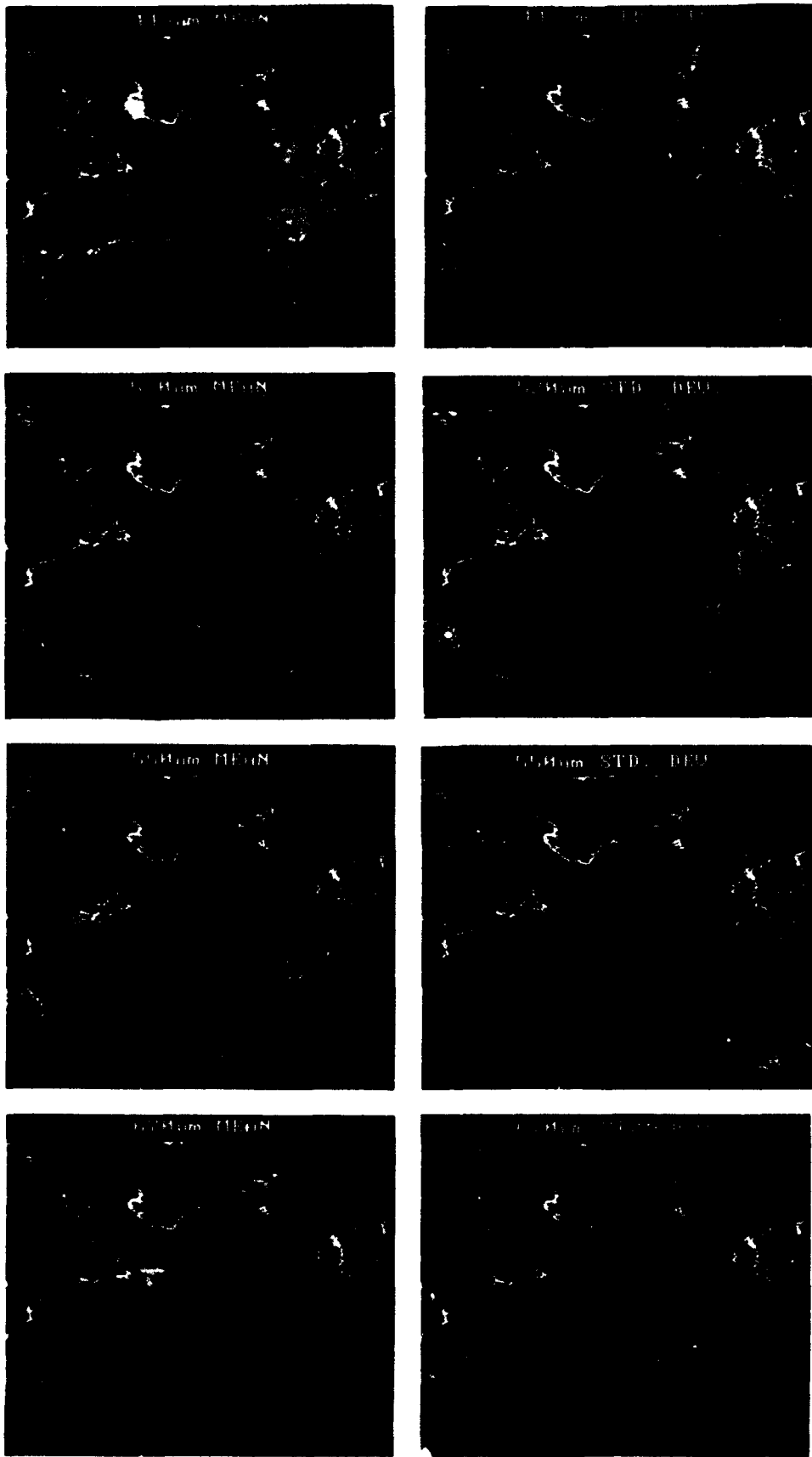


Figure 2. Example of April 1979 products for Region 2.

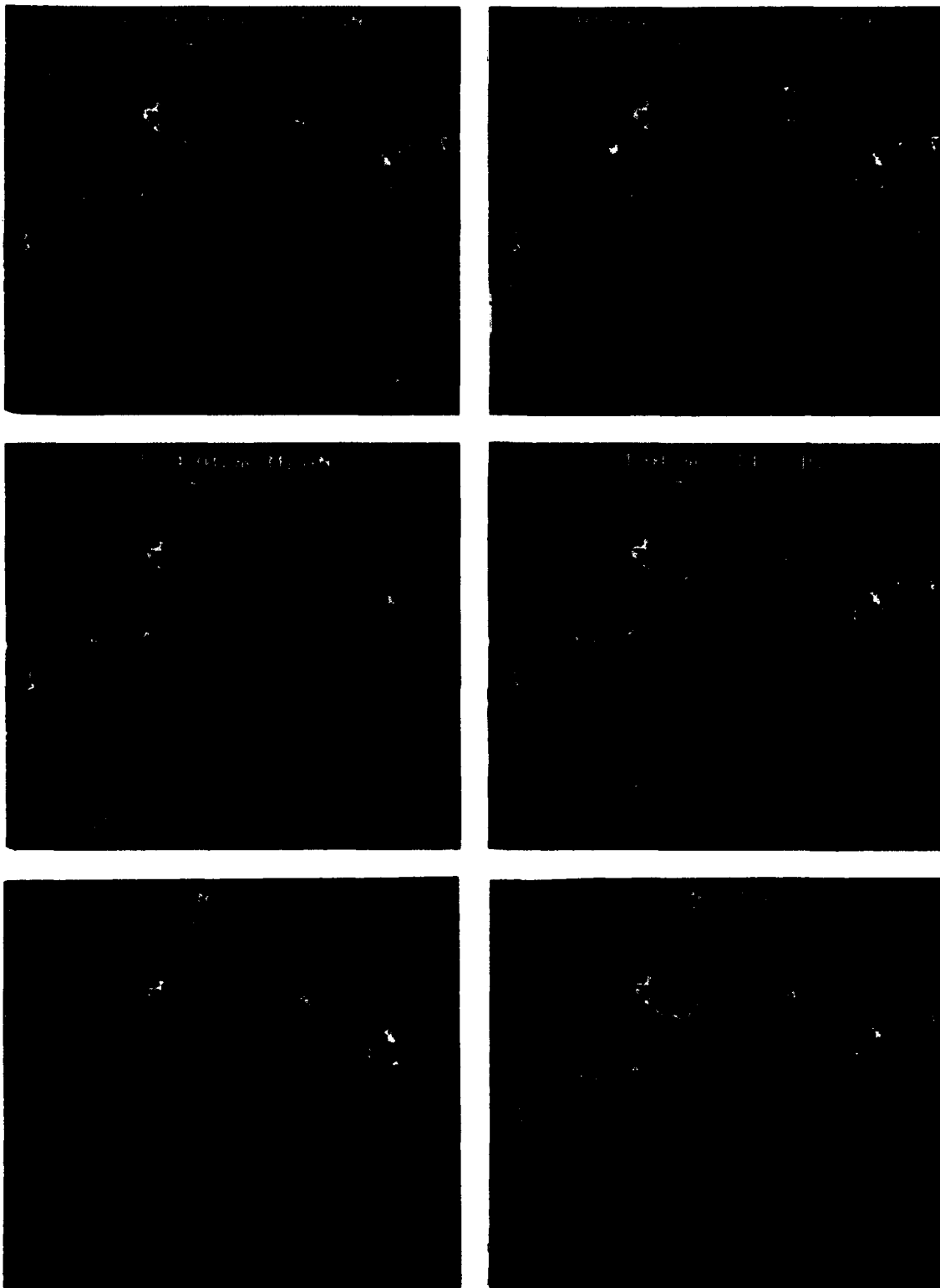


Figure 3. Additional example of products of the database for April 1979.

The monthly composites used to derive the statistics within the 20-km-pixel regions has been shown to be temporally aliased (Abbott and Zion, 1985; Chelton and Schlax, 1991). Useful CZCS ocean color data requires cloud-free conditions and continuous satellite coverage. Because of these limitations, the monthly average products, which are derived in pixel composites, are a consequence of nonuniform temporal coverage for that ocean surface. The averages represent values only when the sun was shining and fortunately the sensor was turned on. The total possible coverage at 30° latitude is approximately 18 scenes a month (based on the satellites repeat coverage). Assuming that within the 20 x 20 km region, complete cloud-free conditions occur, a total of over 400 pixels are possible for each scene. Thus, the total amount of pixels for each 20-km bin that are available for a monthly composite is 7200. This number reduces substantially based on the area's cloud cover and lack of CZCS data availability. As the total pixels available for the 20-km bin are reduced, the averaging is not a true representation of the ocean property in the bin. Note that the average and standard deviation of the bin is characterized by this number of pixels and that this number changes with each 20-km bin and from month to month. However, the wealth of data supplied by the satellite still provides an initial method for estimating the optical climatology. The number of scenes and the total number of pixels from each bin is also available for each monthly composite so that it is possible to determine some confidence as to the number of pixels used in establishing the product.

Follow-on pixel composite techniques are under investigation to eliminate the temporal averaging. Chelton and Schlax, 1991 have examined estimation of time averages from irregularly spaced observations. This technique assumes knowledge of the power spectrum of the time scales of chlorophyll variability and weights the monthly averaged composite accordingly. The overall effect is to reduce the anomalies observed in month-to-month averages. These techniques are presently under investigation and will be incorporated into future satellite databases.

Organization of the Database

The databases reside on a 3.5 gigabyte SONY WORM drive interfaced with a Compaq 386/25 PC computer. The CZCS monthly database is organized utilizing DOS directory structure organized according to year. The "year" is in the root directory with 12 months listed as subdirectories of the year. Within each monthly subdirectory there are 112 files for the regions and products already discussed. Thus, the entire database represents a total of 10,304 files. The file names include the following information: year, month, parameter, mean or standard deviation, and region. An example of the directory structure and the file name are shown below:

Example:

Directory Structure:

```
Y1979-----Jan
              Feb
              .
              .
              Dec ----(file name) 9DEC44M.R1
Y1980
.
.
Y1986
```

File Name Structure:

where

- 9 = year (9, 0, 1, . . . 6) 1979 - 1986
- DEC = month
- 44 = 443 nm
- 52 = 520
- 55 = 55
- 67 = 670
- CH = Chlorophyll
- K4 = k(490
- Bi = Bin
- Sc = Scene
- M, S = Mean or Standard Deviation

Extension:

R1,R8 = Region 1 - Region 2 (Figure 1)

The file structure is set up as a 512 sample x 513 line 8-bit array. The first record of 512 bytes is the header record. The header contains the latitude, longitude coordinates of the image, geographical projection, and the type of product and geophysical data scaling. The records 2 through 513 represent the geophysical data scaled to 8-bit data. Details of the file format can be found in McClain et al., 1990.

Interpretation of the database

The monthly time scale was selected for the optical climatological database because it established the longest time scale in which mesoscale ocean features can easily be observed. This time scale is also able to describe the changes in the solar irradiance and the heating cycle dominant in the ocean that is believed to control the nutrient availability and ultimately the bio-optical climate (Dickey, 1991). Thus, the monthly scale identifies the phytoplankton crop size that is responsible for the optical environment in deep ocean waters. The shorter time scale such as weekly and daily periods, which address physical forcing from storm events, turbulent mixing, and inertial periods, is not represented by the monthly climatology. These physical forcings are more dominant in the coastal environment, and the average optical distribution observed in the coastal environment is characteristically shown to have high variability. Future efforts for an optical database of optical properties should be performed at a time scale of 3 - 7 days in order to capture the higher frequency forcings that control the coastal environment.

The 20-km resolution was selected for the spatial scale of the database as the largest area coverage representing a "large" phytoplankton patch. At this resolution, fronts and eddies are observed in addition to synoptical storms and seasonal cycles of the mixed-layer depth and biogenic cycles.

The effects of spatial and temporal averaging will reduce the detail oceanic features such as the Gulf Stream and Loop Current, but the features are not totally removed and can be identified in the monthly composites. **Figure 4** is a comparison of the high resolution 2-min scene $k(490)$ image off the U.S. east coast on April 24, 1982 with the monthly composite in April 1982. In this example the warm core eddy located to the north of the Gulf Stream is observed as low $k(490)$ values, and is similarly observed in the monthly composite. Low $k(490)$ values associated with the Gulf Stream indicate the approximate position. The April climatology shows the stream departing off the east coast near Cape Hatteras. However, further eastward, the Gulf Stream climatology is observed as irregular and complex and not a continuous ocean structure. This blurring effect occurs because the Stream's dynamic ocean boundaries change within the 1-month periods forming rings and meanders. The monthly average of the ocean structure appear nondistinctive and somewhat fragmented.

The standard deviation product provides an estimate of the variability occurring within the 20-km-pixel region during the month. The standard deviation product (**Figure 5**) of the east coast for April 1982 illustrates the stability of ocean water masses for the monthly time scale. The region south of the Gulf Stream in the Sargasso Sea is shown as a low diffuse attenuation coefficient ($<0.03 \text{ }^{-1}$). Note that the cold core eddy with elevated $k(490)$ values, which is observed in the mean $k(490)$ image, is not observed in the standard deviation image. This indicated that the eddy remained stationary for at least the 1-month period. The standard deviation image product suggests water mass optical

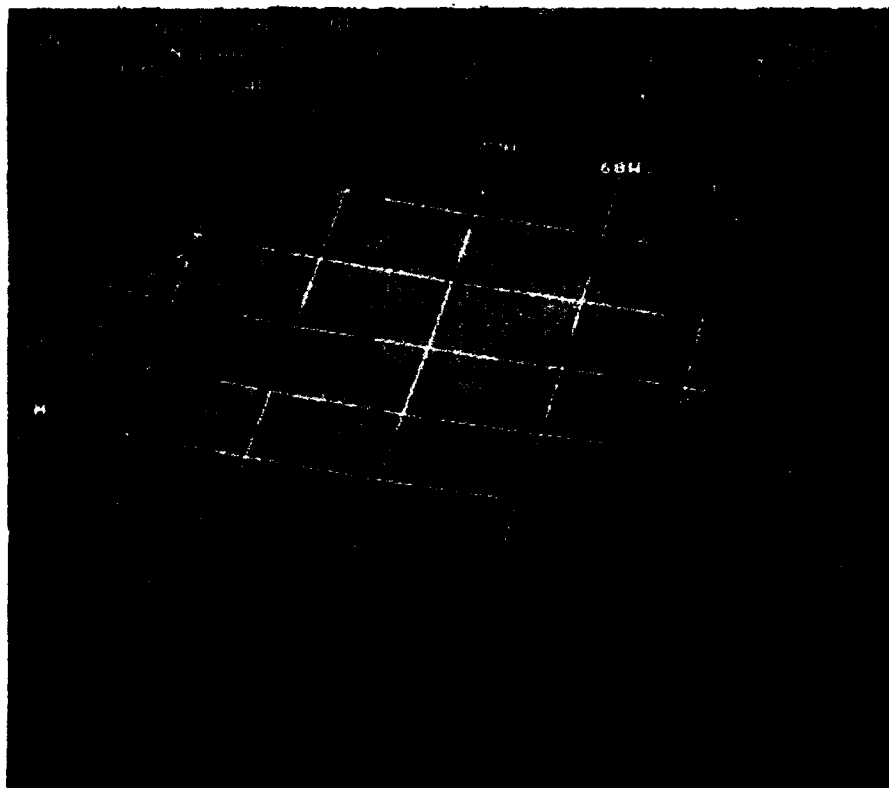
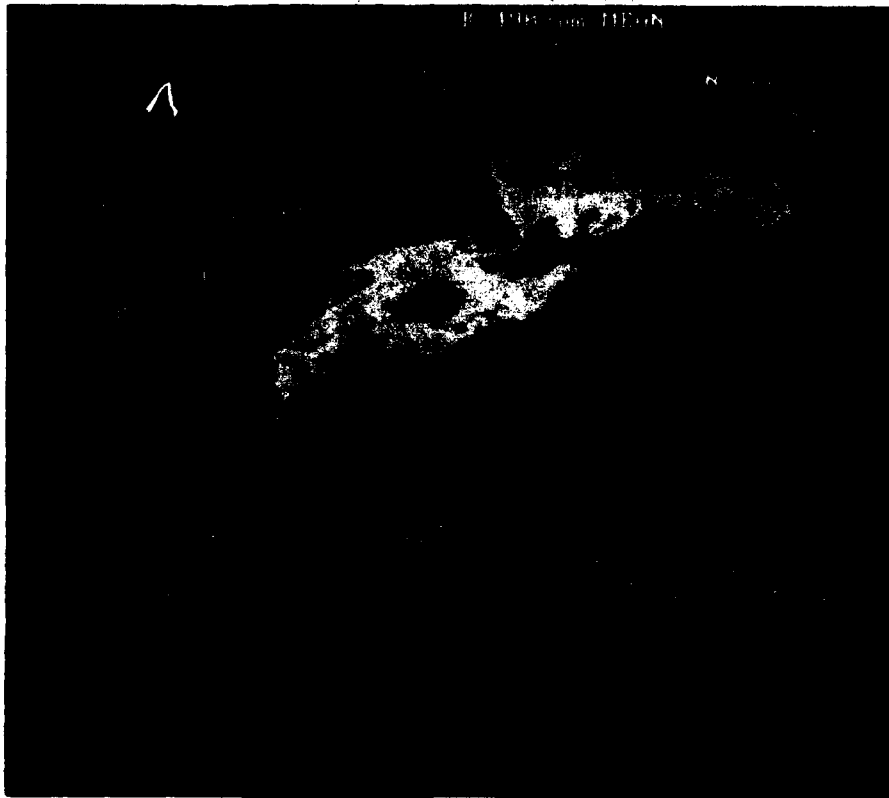


Figure 4. A comparison of the mean monthly k(490) composite (upper) for April 1982 with an individual April 24, 1982 k(490) scene (lower) at a higher (9 km) resolution.

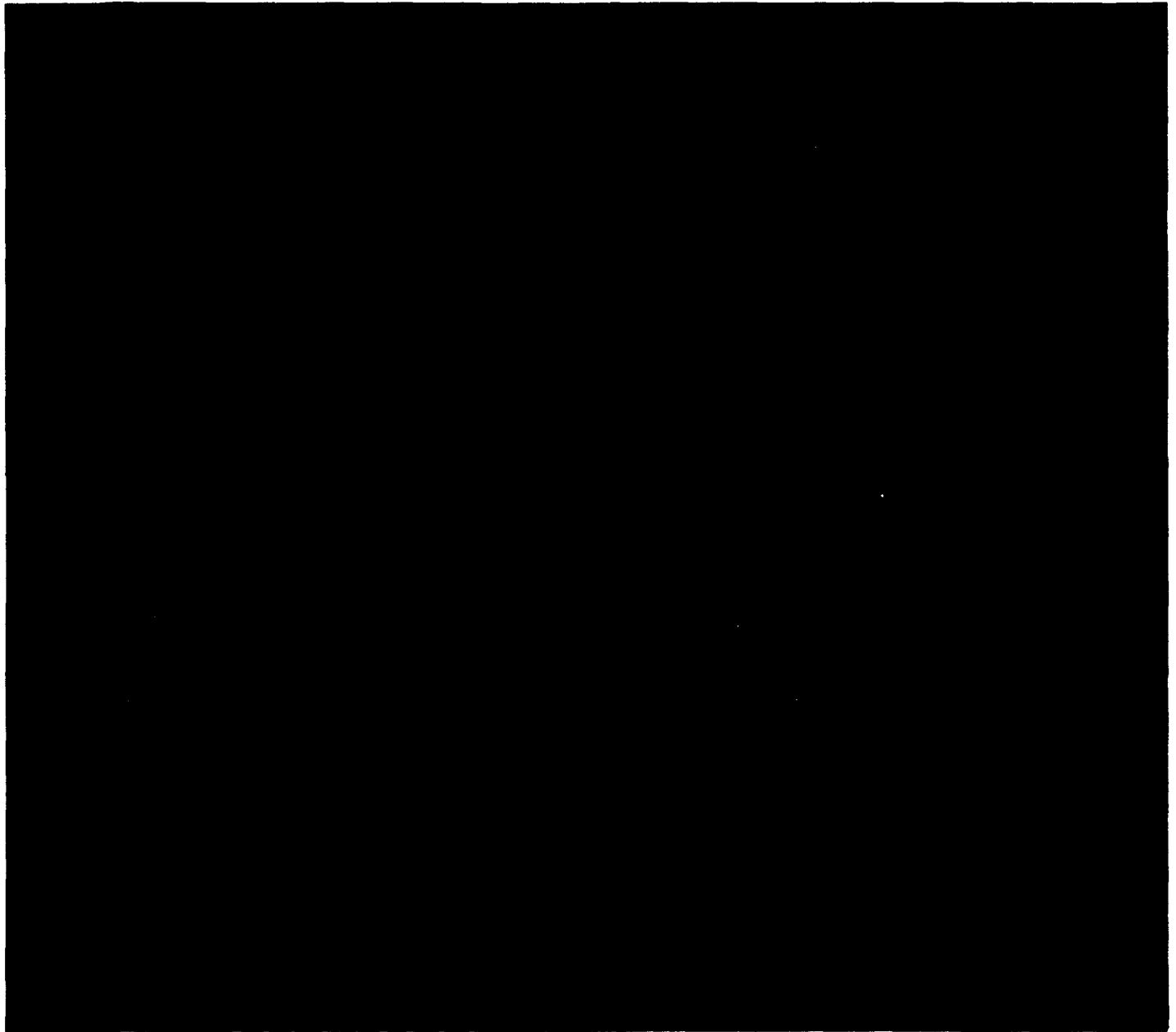


Figure 5. Standard deviation of $k(490)$ for the April 1982 composite shown previously.

stability. Areas displaying high $k(490)$ variability should characterize dynamic ocean regions such as frontal locations and movements of ring structures. Our present understanding of the variability of the optical signature in the surface ocean is limited. Because the ocean color signature and the coincident surface optical properties are controlled by a variety of physical and biological processes, the variability and causes of the variability are difficult to determine. However, correlations such as shown in **Figure 6** show a strong logarithmic relationship between the mean and standard deviation (Arnone and Elenbass, 1991). This trend is observed in other geophysical data and demonstrates the clear need for detrending optical data in order to address the spatial and temporal scales of variability.

OPTICAL WATERMASS CLASSIFICATION

EAST COAST 1979-1986

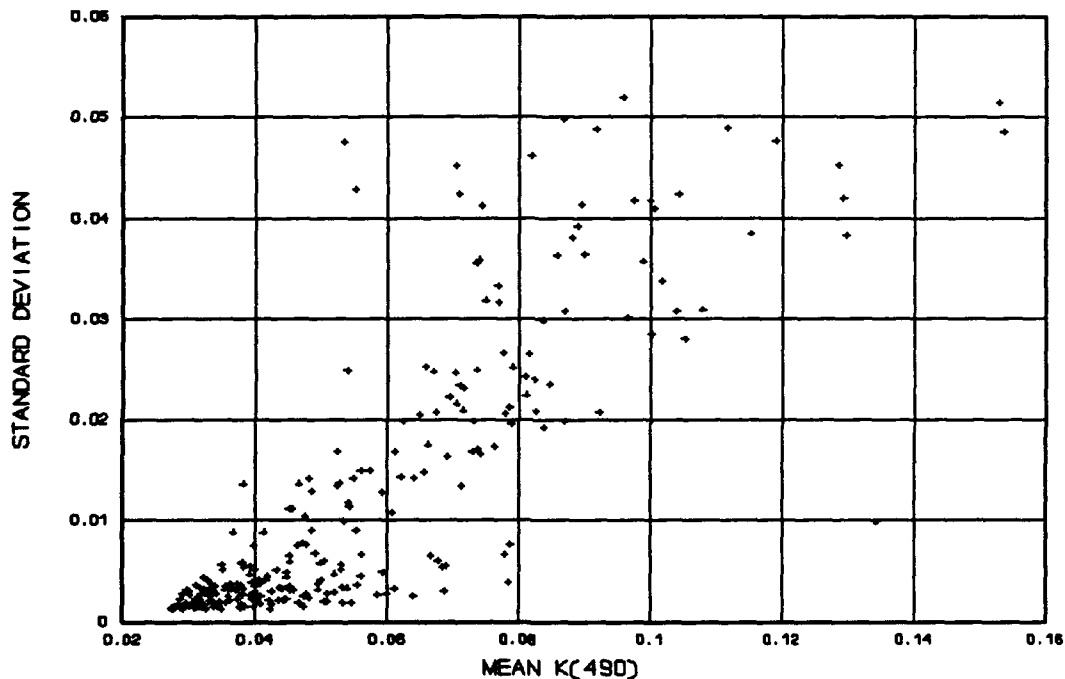


Figure 6. Logarithmic correlation of the mean and standard deviation of optical properties in four North Atlantic regions.

A study of variability of optical properties within selected water masses was performed off the U.S. east coast using the optical database. The 92-month average and variance of areas representing the (1) Sargasso Sea (2) Gulf Stream (3) Slope water, and (4) Shelf Water (**Figure 7**) was determined by examining all $k(490)$ pixels occurring within these four regions (Arnone and Elenbass, 1991). The resulting average $k(490)$ values, representing these areas for each of the monthly composites is shown in **Figure 8**. Notice that the Sargasso values remain low and relatively stable for the entire 92-month period. The Gulf Stream waters, also comparably low $k(490)$ values, show a slight elevation in the spring months corresponding to the spring phytoplankton bloom. The Slope waters show

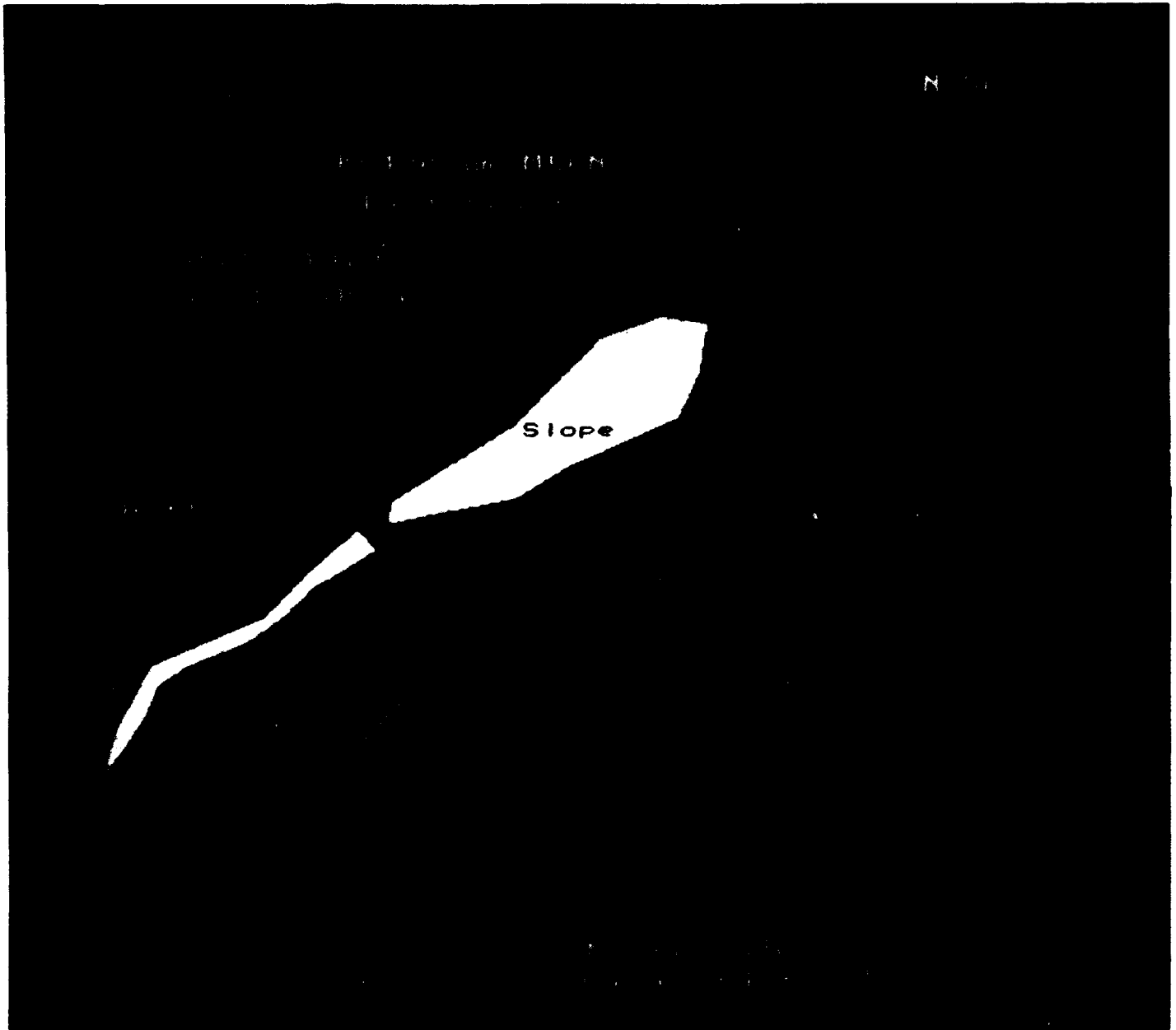


Figure 7. Location of water masses in the eastern U.S. representing Sargasso, Shelf, Slope, and Gulf Stream.

increased $k(490)$ values with an elevated spring period. Finally, the high $k(490)$ values observed in the Shelf waters indicate a 12-month period occurring in the winter-spring period. Physical forcing and the resulting optical variability on the Shelf waters is an interaction of the higher temporal frequency such as the tides and local storms modulating the longer scale seasonal cycle. Spectral analyses of these data showed a dominant 12-month period.

OPTICAL WATERMASS CLASSIFICATION
EAST COAST 1979-1986

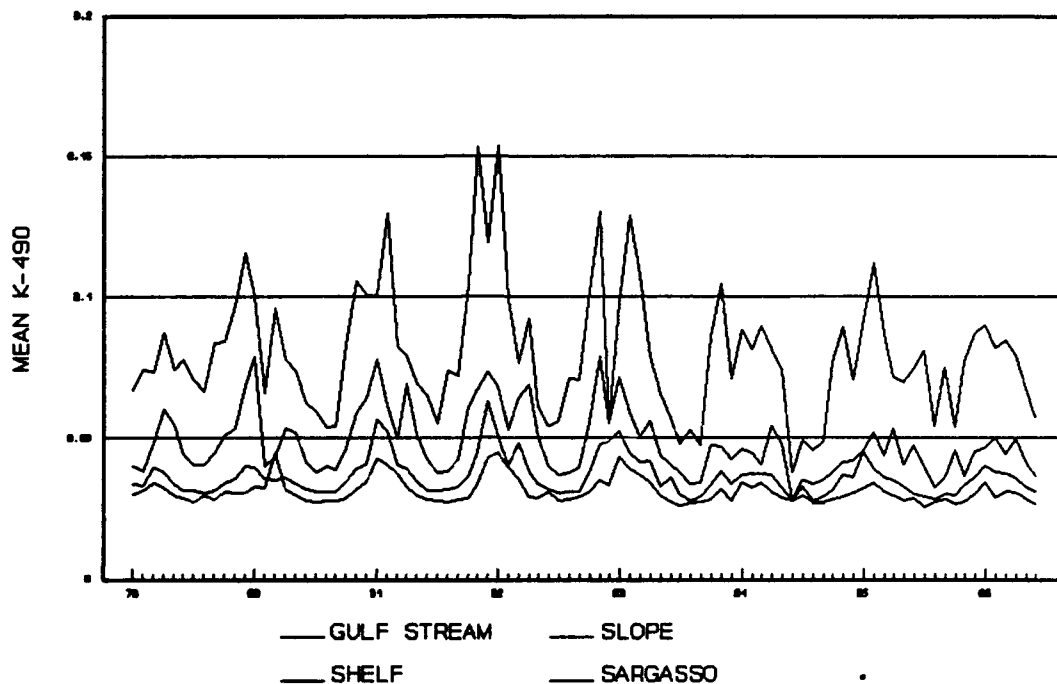


Figure 8. The 92 monthly mean $k(490)$ values for the ocean regions shown in Figure 7. The low $k(490)$ values in the Sargasso Sea suggest the stability of the CZCS ocean color products.

The interannual variability of the optical climatology is shown for the Gulf of Mexico and the southwestern U.S. waters (**Figure 9**). The December 1978, 1979, and 1980 imagery clearly shows changing distribution of the optical climate. The Gulf of Tehuantepec off the west coast of Nicaragua shows the interannual response of the upwelling and the consequential $k(490)$ variability. The 1979 $k(490)$ in this area was weak whereas the 1980 and 1981 response shows marked increase in the $k(490)$ values. Notice also the Gulf of California has elevated $k(490)$ values in 1979 whereas the other 2 years are lower. Other regions show the general climatology is not changing substantially during the 3-year period. The northern Gulf of Mexico coast is shown as consistently high in all 3 years. The climatological database provides a method for characterizing "typical" ocean optical conditions for a region and discriminating whether the optical properties are stable from year to year.

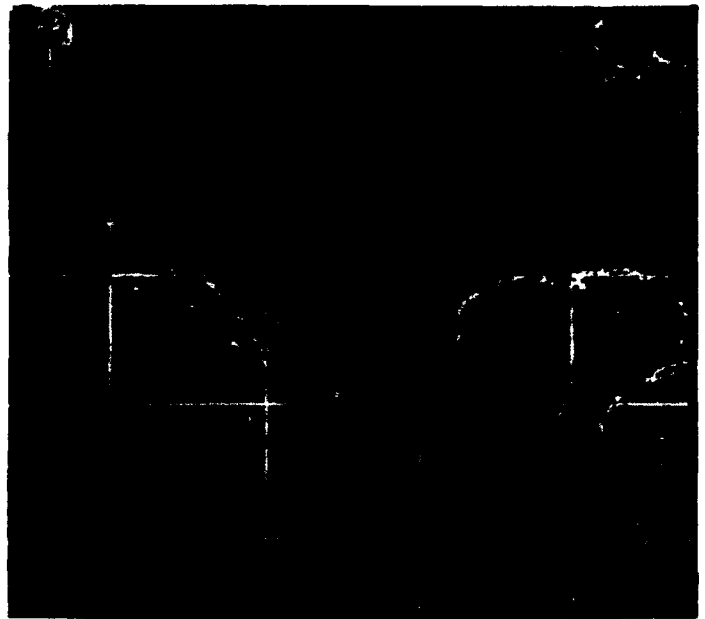
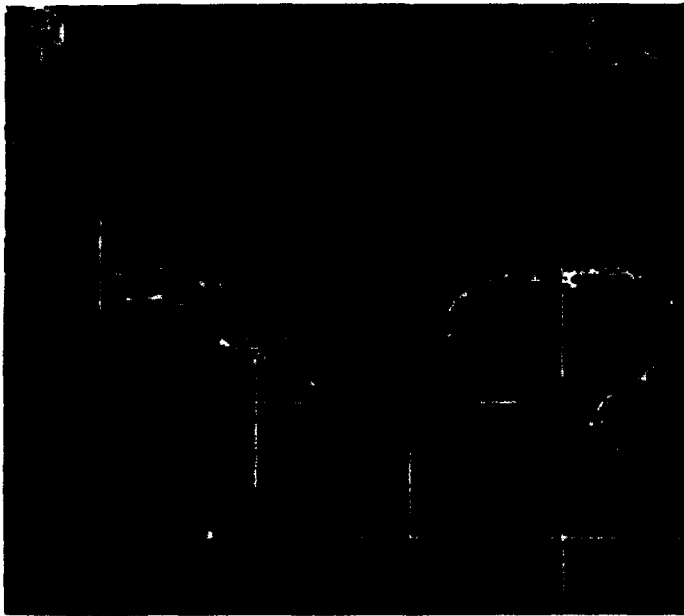


Figure 9. The interannual optical variability of the Gulf of Mexico and southwest U.S. for December 1978, 1979, and 1980.

Ocean optical processes occur in response to physical forcing that has different seasonal time scales. The four season forcing occurring in the North Atlantic is contrasted with two seasons occurring in the Arabian Sea. The effects of the Monsoon Season on the optical properties are observed in the optical climatology of the Persian Gulf (**Figure 10**). The development of the Monsoon in October, which produces a strong southwestern wind and heavy rain, results in increasing high $k(490)$ values in the Arabian Sea. Continued development of the Monsoon shows peak $k(490)$ values occurring in November (Arnone and Oriol, 1991). The annual Monsoon influences the physical circulation in this region in addition to an overturning of the surface waters and deepening of the mixed layer. The resulting increase of nutrients in the surface waters produces increased $k(490)$ values as a response of phytoplankton production. A steady decline in $k(490)$ values is observed from December through April as the Monsoon declines and the nutrient supply declines. Stratification of the water column occurs in June during the dry season and the $k(490)$ values are low in the ocean waters. The changing distribution and the influence is observed in the monthly database sequence. The optical database provides an initial procedure for examining an unknown ocean region to determine the seasonal response of the optical regime.

Validation of the Optical Database

The validation of the $k(490)$ products is difficult to access since the accuracy is largely controlled by accurate atmospheric elimination that is regionally and seasonally dependent. Generally, areas where a continental air mass (U.S. east coast) prevails have less accuracy than the maritime air mass regions (U.S. west coast) because of non-uniform aerosol character. In the Middle East region the aerosols associated with dust storms will influence the accuracy of the $k(490)$ products. Quantifying these errors is a major problem and perhaps can only be addressed through comparison with the limited in situ observations available.

Additionally, the CZCS $k(490)$ accuracy is degraded in coastal waters (Arnone, 1983; Smith and Wilson, 1981) because of (1) improper atmospheric correction and (2) inadequate sampling of high variability.

Chlorophyll Validation

The validation of the CZCS optical database was examined by comparison of CZCS products with in situ ship observations. The availability of ship measured $k(490)$ during the CZCS operation was highly limited. An Initial comparison has therefore been performed by comparison of chlorophyll data because there are more ship chlorophyll data available. A validation study of the correlation of ship measured chlorophyll and CZCS derived values has been conducted by Lohrenz et al., 1988; Martinez et al., 1990; Gordon et al., 1980; Esaias, personal communication, 1991; Balch et al., 1991; Arnone

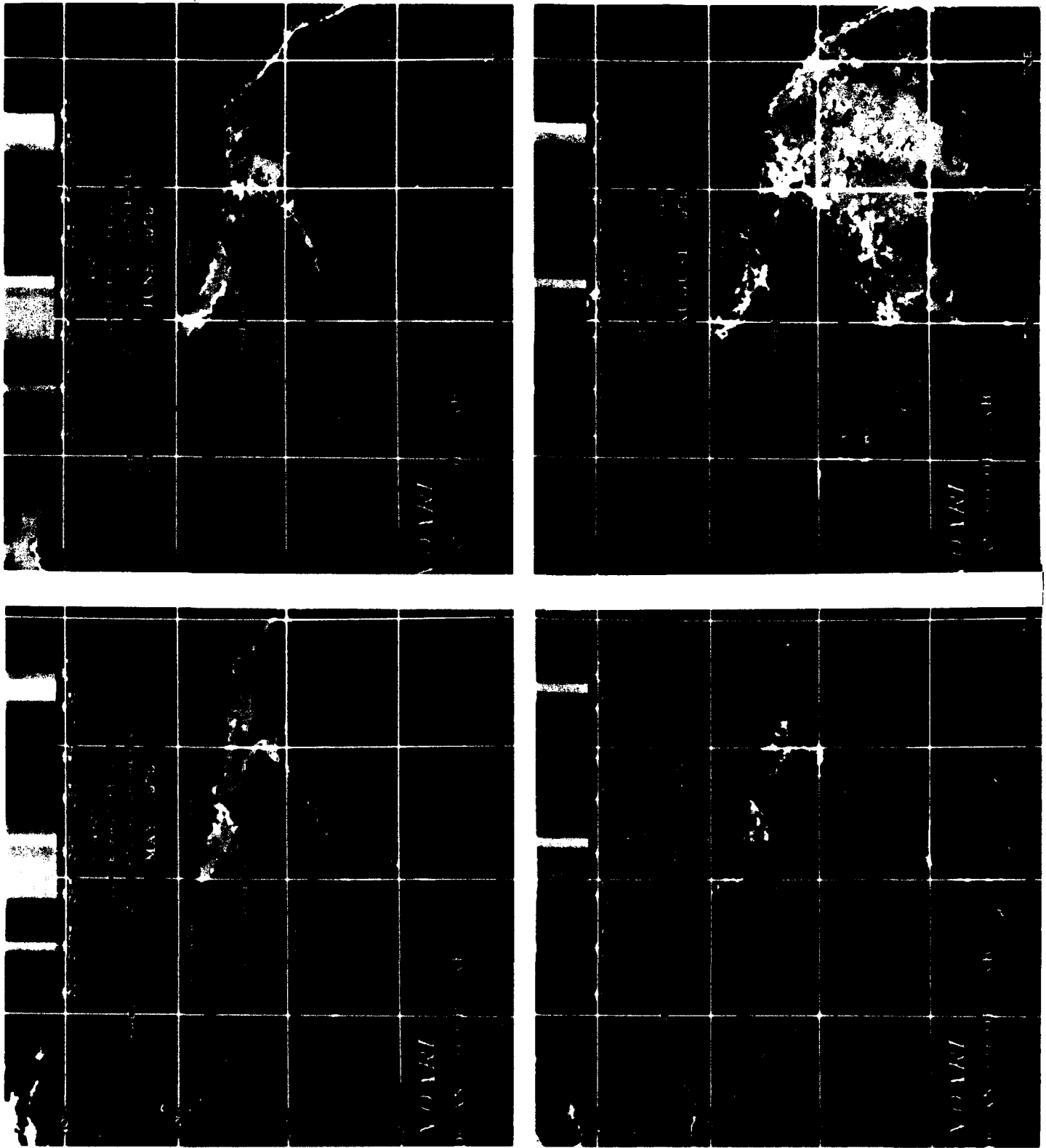


Figure 10. The effect of the Monsoon on the Arabian Sea optical climatology. The elevated $k(490)$ values are observed at the onset of the Monsoon in August. The dry season (June) is characterized by low $k(490)$ values. 20

et al., 1991c. These studies were based on the large amount of chlorophyll data available in oceanographic cruises. An accuracy of 85% between ship and satellite chlorophyll have been achieved in the Mediterranean (Lohrenz et al., 1988; Martinez et al., 1990).

Esaias' data set represent approximately 700 data points distributed around the world characterizing the "deep" Case 1 water masses. The correlation of these data with coincident CZCS data observed within a period of 24 h with ship observations had a correlation coefficient (r^2) value of 0.90 (Figure 11).

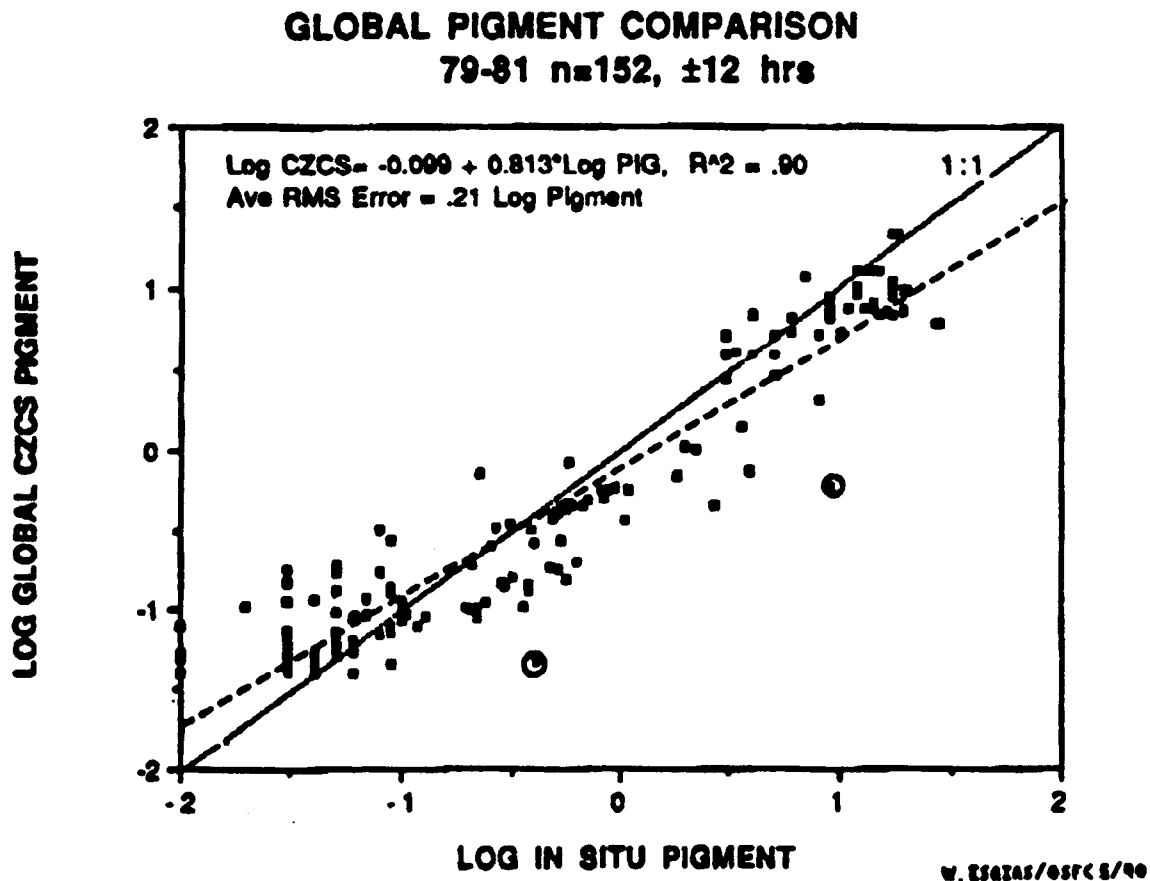


Figure 11. Comparison of log ship vs satellite chlorophyll (from Esaias, 1986).

Balch's data set represents 731 chlorophyll data points collected from October 1978 to May 1986 from global open ocean areas (Figure 12). This ship data is compared with the

20-km CZCS data set, achieved by NASA (Goddard Space Flight Center). Integrated ship chlorophyll within the first attenuation length was compared with near coincident (+/- 1 day) integrated CZCS derived chlorophyll (Clark, 1981; Gordon and Clark, 1980a). **Figure 13** illustrates the log ship vs. log satellite derived pigment to have a coefficient of correlation (r^2) of 0.40. The resulting equation, $C_{sat} = 0.60 * C_{ship} - 0.14$ implies that the satellite estimates are consistently **overestimated**.

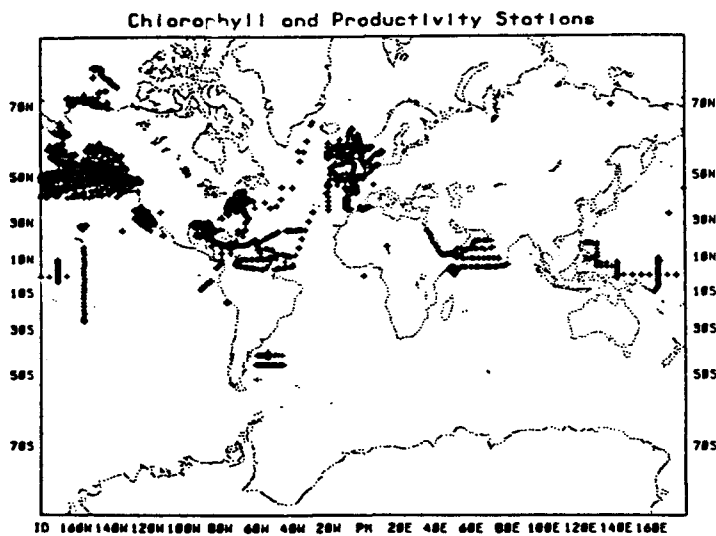


Figure 12. Locations of stations used in comparison of ship and satellite chlorophyll (Balch et al., 1991).

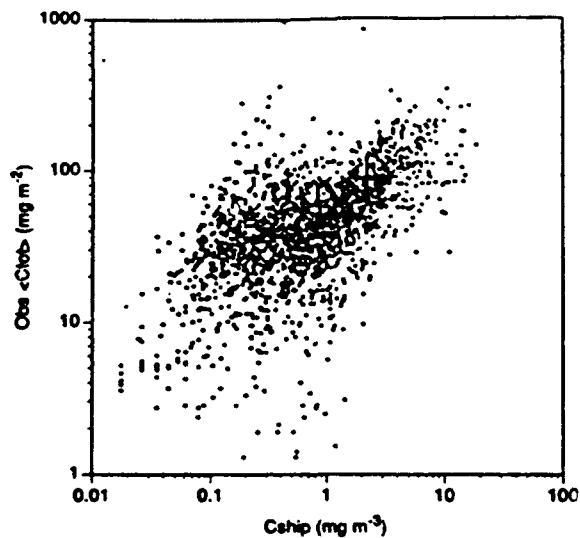


Figure 13. Correlation of 731 ship stations and satellite chlorophyll points ($r^2 = 0.4$).

Arnone et al. (1991c) data set used ship measured coastal chlorophyll concentrations, in estuaries and coastal waters in the Chesapeake and Delaware Bay, and along the gulf coast of U.S. waters. These data were compared with the **mean monthly climatology** from the optical database for the 20 km² regions. Thus, this comparison used temporally and spatially averaged CZCS chlorophyll data for comparison and **not** near time coincident comparison as was previously shown. Surface chlorophyll from the SEAMAPS data set (NOAA, National Marine Fisheries) represents approximately 2281 data points from the east and gulf coasts of U.S. waters. These ship and satellite derived chlorophyll data were converted to $k(490)$ using Morel et al. (1988):

$$(4) \quad k(490) = kw(490) + \epsilon(490) \text{Chl } e^{(490)}$$

$$\begin{aligned} \text{where} \quad & kw(490) = 0.0217 \\ & \epsilon(490) = 0.0690 \\ & e^{(490)} = 0.702 \end{aligned}$$

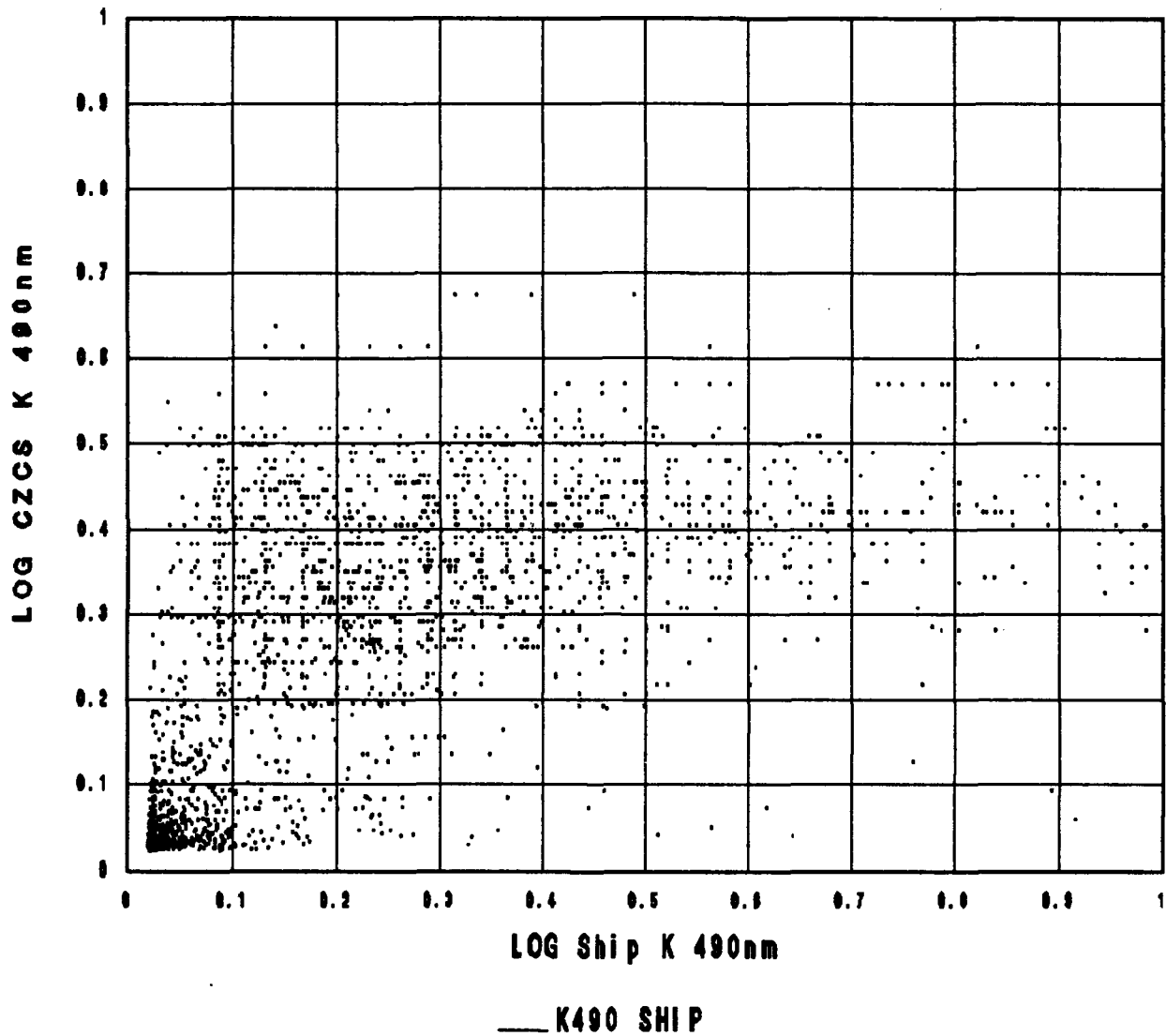
The results of log ship and satellite chlorophyll comparison was shown to have a correlation coefficient (r^2) values of 0.5 (**Figure 14**). The equation is shown to be:

$$k(490)_{\text{sat}} = k(490)_{\text{ship}} * (0.614) - 0.181$$

From this relationship the satellite appear to overestimate the low $k(490)$ while the upper end ($k > 0.1$) appears accurate. At k values $> 0.5 \text{ m}^{-1}$, the satellite under predicts the value.

A comparison of the optical database with ship data collected along a 750- km track in the North Atlantic shows good agreement. **Figure 15** shows the location of the ship track in May and June 1979 (Gordon et al., 1983). Surface chlorophyll concentrations were obtained starting in the open North Atlantic and extending through a warm core ring and into the coastal waters off Woods Hole, MA. Surface chlorophyll values collected were converted to $k(490)$ using equation 4 (Morel, 1988) and plotted in **Figure 16**. Also shown in this figure are the converted chlorophyll to $k(490)$ for (1) the satellite data from the June 9 and 10 image coincident with the cruise and (2) the monthly average $k(490)$ values from May and June 1979. All profiles clearly show the presence of the low $k(490)$ values of the warm core ring. Upon entering the coastal shelf waters the variability of the $k(490)$ increases substantially and comparisons of ship and satellite are more difficult to access because of the space and time scales of optical variability. The monthly composites are slightly higher than ship values.

SEAMAP CRUISES '82, '84, '85 AND '86
CHESAPEAKE BAY CRUISES '84-'86



$r^2=0.409$
TOTAL POINTS=2201

Figure 14. Comparison of log ship vs. satellite chlorophyll from SEAMAP and Chesapeake Bay (Arnone et al., 1991).



Figure 15. The ship track position overlaid on CZCS k(490) composite for June 1979.

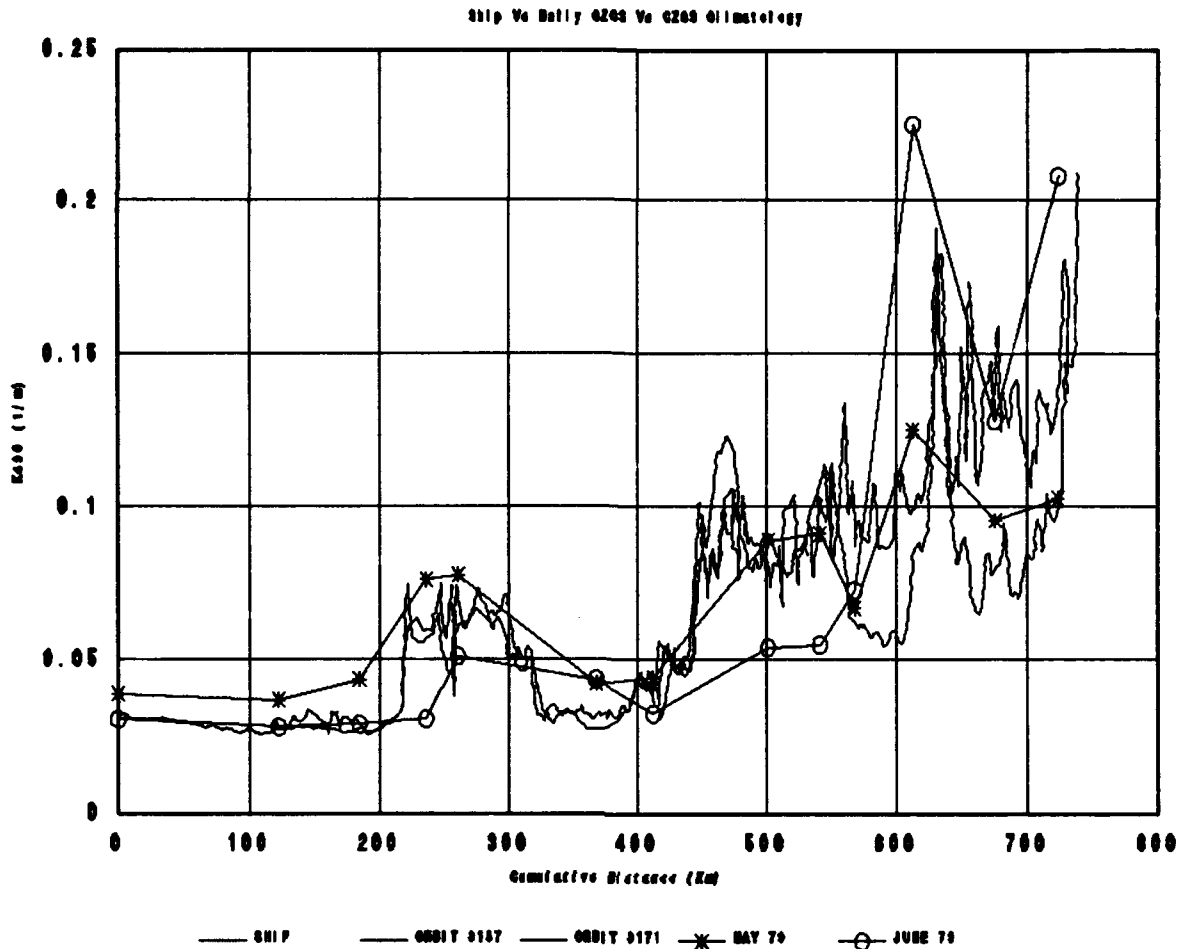


Figure 16. Comparison of ship and satellite data extending from open ocean through a warm core ring into coastal waters.

Diffuse Attenuation Coefficient Validation

The previous comparison examined validation of the optical properties from the database through converted $k(490)$ from chlorophyll. The chlorophyll to $k(490)$ relationship has been established for Case 1 water to have a correlation of 0.82 (Austin and Petzold, 1980; Morel, 1988). Thus, there is inherent error simply in this comparison. The relationship of water leaving radiance to $k(490)$ established by Austin and Petzold, and extended into Case 2 waters by Mueller et al. (1991) is valid for a variety of $k(490)$ values. The error of accuracy (i.e., problem) is not with this algorithm but with the satellites ability to estimate water leaving radiance in Case 2 waters. In Case 2 waters, the relationship using spectral water leaving radiance should be better for $k(490)$ than for chlorophyll. Chlorophyll is a biological process and in coastal regions (Case 2 waters) is not coupled with optical properties. Spectral water leaving radiance and $k(490)$ are optical properties that are separate from chlorophyll concentration. Thus, correlation between ship and CZCS chlorophyll comparison will NOT BE AS RELIABLE as the

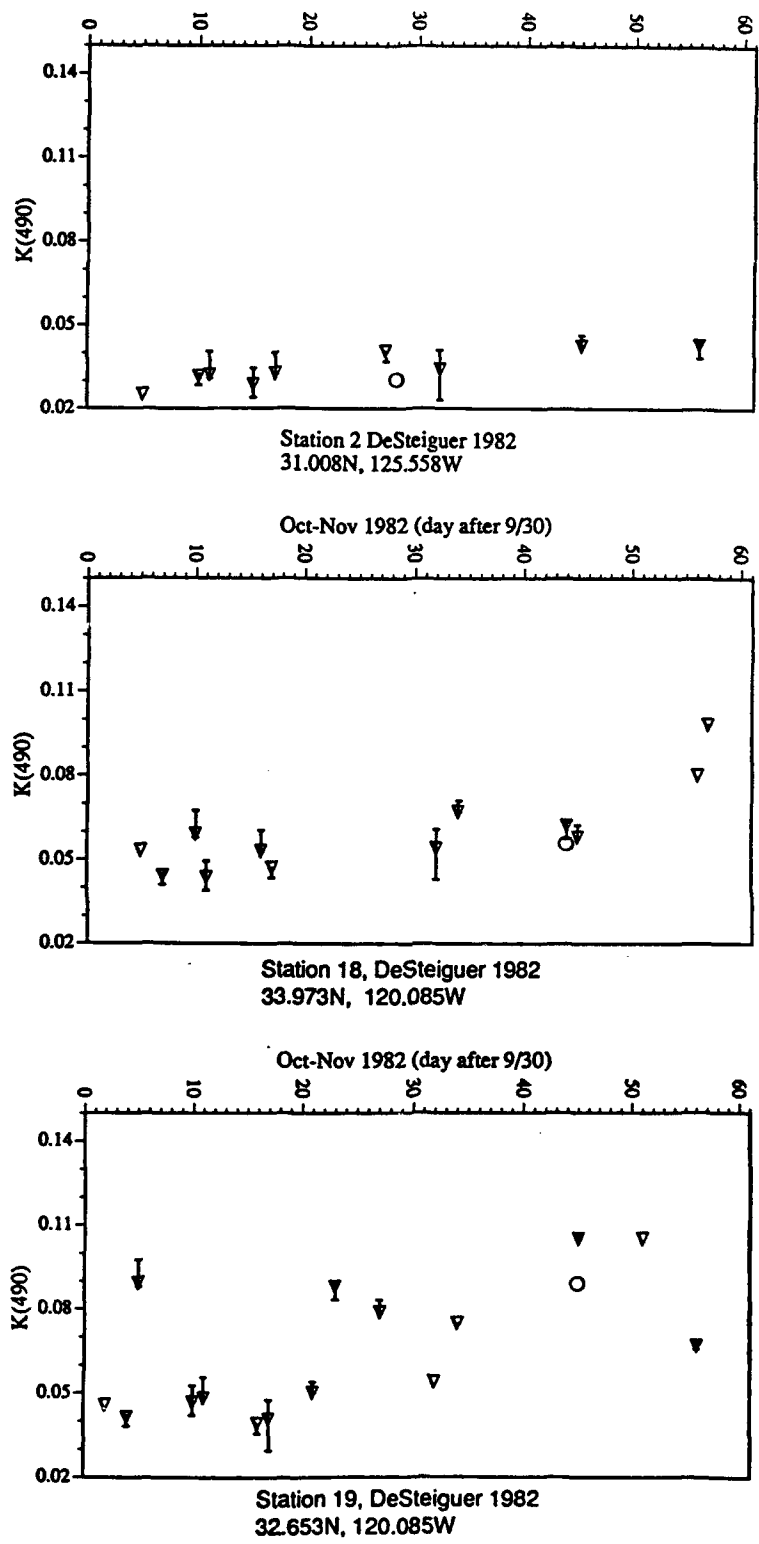


Figure 17. Comparison of ship $k(490)$ data (circles) with CZCS $k(490)$ (triangles) for three different water types off the U.S. west coast (Mueller, personnel communication).

correlation between ship and CZCS k(490) comparison.

Mueller (1991) (personal communication) has shown a strong correlation of CZCS and ship k(490) for the data set off the U.S. west coastal in Case 1 waters. **Figure 17** shows the ship measurements of k(490) compared to k(490) values retrieved from the satellite during a 60 day period in October and November 1982. The circles represent actual ship k(490) measurements for the first attenuation length collected on specific days. The triangles represent a 16- km average of the daily k(490) computed for that day at the station location with the spatial variance represented by the bars. The daily variation of k(490) is illustrated by the satellite derived k(490) for three time periods at three locations. The CZCS calculated k(490) is shown to be reasonably within the limits of the ship measurements. The first water mass represent k(490) values of 0.03, the second representing values of 0.055, and the third representing values of 0.09 m^{-1} . Arnone et al. (1991c) examined a comparison of ship spectral attenuation coefficient data set in the Gulf of Maine (Bigelow data set) with monthly CZCS k(490) data. Diffuse attenuation coefficients for 74 ship data points were available at four separate wavelengths 440, 520, 550, and 670. The satellite k(490) data were converted to these wavelength using Austin and Petzold (1984). The log of satellite and ship data are shown (**Figure 18 a-d**) to have regression coefficients (r^2) of 0.67, 0.62, 0.57, and 0.33 for the four wavelengths. The regression is hinged about a k value of 0.1 where values below the satellite overestimates and values over the satellite underestimates.

Satellite k(490) values were compared with ship data in the Persian Gulf. Seventeen k(490) values in the Persian Gulf collected in September 1987 were compared with average September k(490) values derived from satellite from 1979 to 1983. **Figure 19** shows a plot of the log in situ and satellite k(490) values for the same locations. The regression coefficient is 0.60 and indicates that the satellite derived k(490) tend to underestimate the measured k(490) values especially in high values. However, because of the extremely high variability observed in turbid water regions, which are impacted by events such as the tidal cycle and local storms it is difficult to assess whether the inconsistencies are caused by inaccuracies in the CZCS algorithm or in the sampling (time and space). Future investigations must examine these optical scales of variability in the coastal environment.

Figure 18. Ship spectral diffuse attenuation coefficient data from the Gulf of Maine are compared with monthly satellite k data. The satellite k(490) was converted to k at the ship wavelength. The regression coefficients of 0.67, 0.62, 0.57 and 0.33 were found for each wavelength (443, 520, 550, and 670 nm) (Arnone et al., 1991).

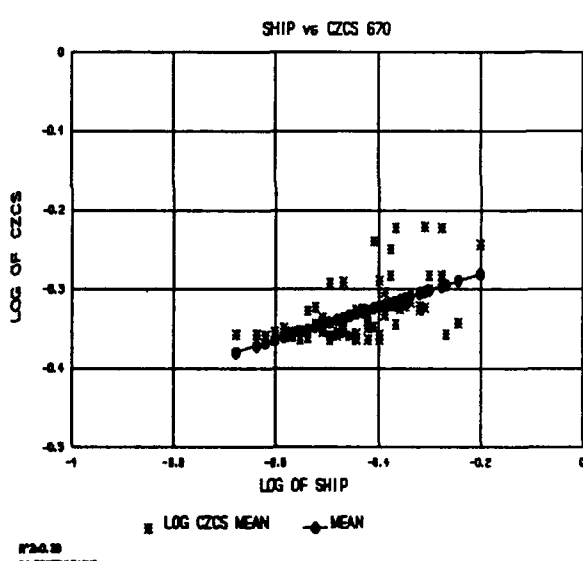
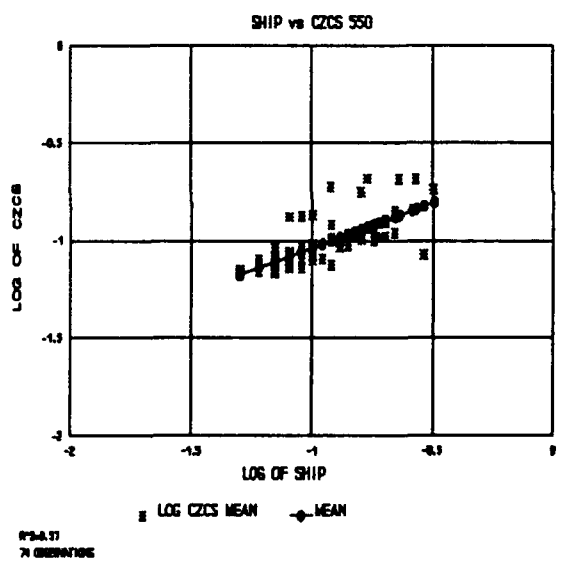
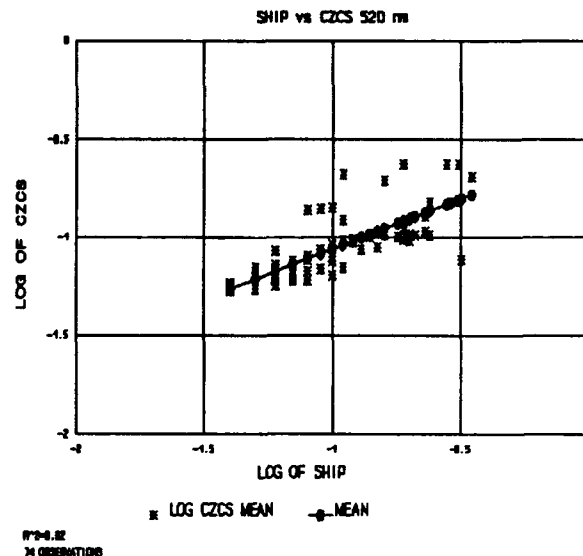
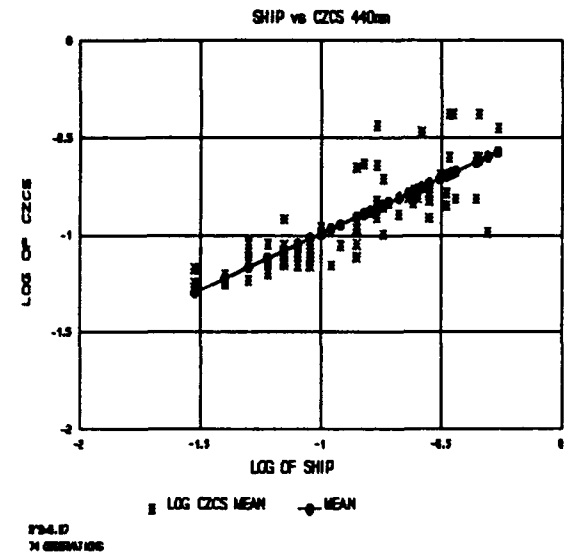
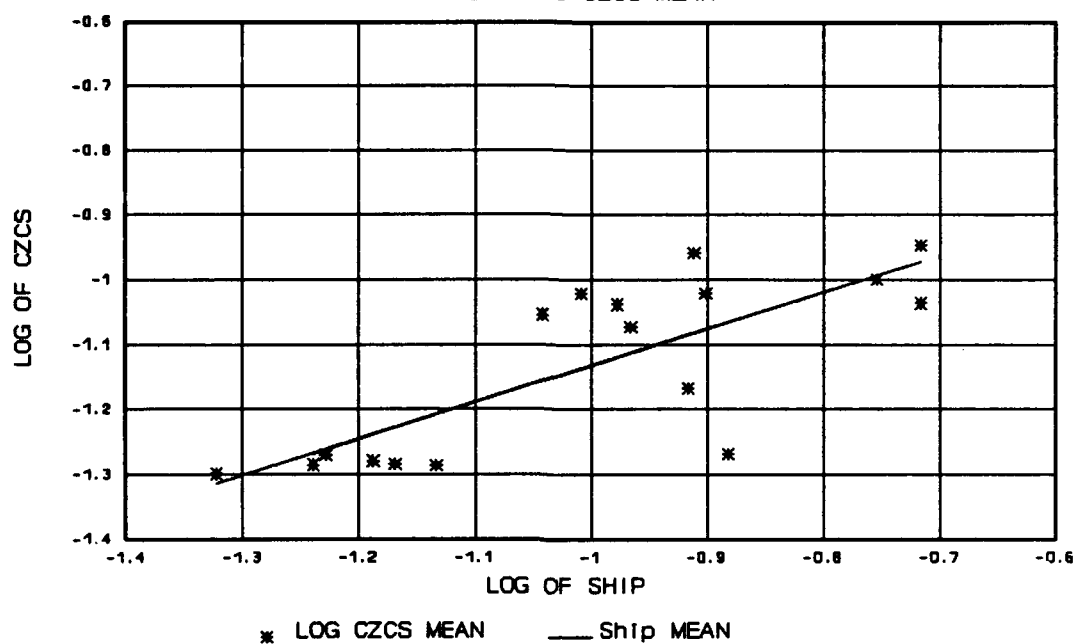


Figure 18. Ship spectral diffuse attenuation coefficient data from the Gulf of Maine are compared with monthly satellite k data. The satellite $k(490)$ was converted to k at the ship wavelength. The regression coefficients of 0.67, 0.62, 0.57, and 0.33 were found for each wavelength (443, 520, 550, and 670 nm) (Arnone et al., 1991).

PERSIAN GULF CRUISE SEPTEMBER 1987

SHIP vs CZCS MEAN



$R^2=0.60$
17 OBSERVATIONS

Figure 19. Log ship vs. satellite k(490) in the Persian Gulf.

Database Coupling

The future efforts in optical climatology are focused at understanding how the surface optical environments are coupled with other oceanographic forcing and databases. A effort has begun to establish a coregistered database of several ocean properties that are believed to influence the optical distribution. Through examining the covering response of the optical distribution with these other databases, a more complete understanding of optical processes can be developed for predictive modeling.

The ocean optical environment is strongly coupled with the biological activity, i.e., chlorophyll in Case 1 waters. Growth and decay of the chlorophyll in the surface waters is influenced by the availability of (1) light and (2) nutrients. Light limitations are being coupled with the chlorophyll and optical database by determining the monthly solar irradiance distribution at the sea surface (Terrie et al., 1991; Arnone et al., 1991b, c). A model has been constructed using the CZCS aerosol path radiance and the rayleigh scattering to describe the total irradiance at 490 nm for identical pixel locations (20 x 20 km) as the optical database. A coupled 6 year monthly distribution is being examined to characterize the role that light availability has on the optical properties (Arnone and La Violette, 1991; Arnone et al., 1991a, b). Through combining the average solar irradiance at the sea surface with the average k(490) in the upper ocean, predictions of the radiation

at depth can be estimated. Estimating the chlorophyll growth processes are coupled with vertical distribution of the solar irradiance. Models extending the chlorophyll concentration below the surface are being examined.

The sea surface temperature (SST) database is being constructed from thermal IR satellite data from AVHRR. The SST data was processed by the Universities of Miami and Rhode Island and is distributed to NASA Ocean Data System (NODS) by the Jet Propulsion Laboratory. NOARL's Ocean Color Laboratory is assimilating these data into a database coregistered with the optical database to examine the coupling of the SST and optical character of the ocean.

The mixed-layer depth is believed to have significant influence on the vertical optical properties. A mixed-layer depth database is being constructed using the Geophysical Data Environmental Model, GDEM, from the Naval Oceanographic Office, which will be coregistered with the optical database. GDEM represents average seasonal models of the vertical density structure based on all available, vertical CTD and XBT ship observations at a spatial resolution of 5 min. The coupling of these data will provide an initial effort toward estimating the vertical flux of nutrients associated below the mixed-layer depth with the surface optical properties. Regional dependence of the vertical $k(490)$ properties is believed related to this database. GDEM represents the climatological mixed-layer depth on a longer time scale (seasonal average) than the optical database. Improved models for hindcasting the mixed-layer depth are available, which are forced by the heat flux and the surface winds. Mixed-layer-depth models are planned to be executed for time periods coincident with the optical database. This should improve our understanding of how the depth of the mixed layer impacts the optical environments.

The interaction of these databases is directed at providing a realistic prediction of the ocean optical environment. The satellite ocean color climatology provides the foundation of the optical distribution, and the physical and biological process provide an interactive model to extend these surface observations below the surface. The relational database coupling should provide the Navy with an improved understanding of the coupling of ocean processes and should also improve our predictive capability in the optical environment.

The future ocean color satellite planned for the December 1993 launch is the SeaWifs satellite (Hughs, 1987). This satellite has improved spectral channels, dynamic range (10 bits) and calibration features. SeaWifs should continue to supplement the CZCS optical database described here and provide both improved (1) spatial resolution (4 x 4 km) and (2) temporal resolution (global coverage every 2 days). The optical climatological database will be further enhanced through this satellite. Plans to incorporate these data into this optical database are underway. This evolving effort will enable prediction of the oceans' optical character for naval applications.

Conclusions

A database has been compiled using ocean color satellite data to characterize the spatial and temporal variability of the **surface** ocean optical diffuse attenuation coefficient at 490 nm. These data represent the "optimum" optical data for describing ocean variability; however, it has inherent limitations and assumptions. These optical derived measurements should not be assumed to extend vertically into the ocean. Models, which couple physical and biological processes to extend the surface optical properties, are under development. The optical database represents a "CLIMATOLOGY" on a monthly time scale. The user can extract from the database the average conditions occurring within a monthly period. In dynamic ocean regions, the optical signature changes rapidly in response to different water masses and local ocean and atmospheric events. In these areas, the optical properties may be different than predicted by the optical climatology database. This database should be used to establish a "baseline" for the global optical environment. Further implementation of the database is required into predictive optical models. Real time satellite capability offers significant advantages in support of real-time optical prediction.

This optical climatology serves naval applications through supporting planning operations (Pressman et al., 1989). The optical environment impacts several navy electro-optical systems. Understanding the environmental optical constraints on these naval systems could not be performed without this database. This database represents our "best" naval understanding of ocean optical variability presently available. Present naval applications of the optical database are the following:

1. Coastal Optics Planner - The planning of hydrographic operations occurring in the coastal environment such as (1) laser bathymetry (2) mine warfare (3) amphibious assault and (4) coastal warfare.

2. Recognition of watermasses - Recognition of ocean fronts and eddies through their optical signature provides Antisubmarine Warfare (ASW) with an understanding of location of mesoscale events.

3. Improved numerical models - Physical oceanographic models used to predict the mixed-layer depth require forcing of heat distribution with depth. The optical properties improves these model predictions that support ASW operations.

4. Laser propagation models - The performance of the laser system is severely impacted by the ocean optical environment.

References

- Abbott, M.R. and Zion, P.M. (1985). Satellite Observations of phytoplankton variability during an upwelling event. *Cont. Shelf Res.* 4: 660-680.
- Arnone, R.A. and La Violette, P.E. (1991). A Methodology to Determine the Ocean Biological Climatology Using Regional Database Models. International Leige Colloquium on Ocean Hydrodynamics.
- Arnone, R.A. (1983). Evaluation of CZCS and Landsat for Coastal Optics and Water Properties. 17th International Symposium of Remote Sensing of Environment, Ann Arbor MI, May 9-13.
- Arnone, R.A., Oriol, R.A., Trees, C.C., Mueller, J.L. (1990). Bottom Reflectance Discrimination Using Water Leaving Radiance from Coastal Zone Color Scanner. *Ocean Optics X*, Vol. 1032 Orlando, Florida., SPIE p. 597-611.
- Arnone, R.A. and Oriol, R.A. (1990). Ocean Optical Climatology for Middle East Waters. Naval Oceanographic and Atmospheric Research Laboratory, SSC, MS NOARL Technical Note 91.
- Arnone, R.A. and Elenbass, W. (1991). Optical Variability off the East Coast Using CZCS Data. *EOS Trans.* Vol. 72 No. 17 April.
- Arnone, R.A., Terrie, G., and Oriol, R.A. (1991a). Response of Surface Chlorophyll to Solar Irradiance in the Western Mediterranean. IUGG/IAPSO, Vienna, Austria, 11-23 August.
- Arnone, R.A., Terrie, G., and Oriol, R.A. (1991b). Coupling Surface Chlorophyll and Solar Irradiance in the North Atlantic. *Marine Technology Society*, New Orleans, LA Oct. 1991.
- Arnone, R.A., Oriol, R.A. and Terrie, G. (1991c). Validation of CZCS k(490), in preparation.
- Austin, R.W. and Petzold, P.J. (1980). The determination of the diffuse attenuation coefficient of sea water using the coastal zone color scanner. *Oceanography from Space*, ed. J. F. R. Gower, Plenum Publishing Corporation, p. 239-256.
- Austin, R.W. and Petzold, T.J. (1984). Spectral dependence of the diffuse attenuation coefficient of light in ocean waters. *Ocean Optics VII*, Vol. 489 SPIE p. 168-178.
- Balch, W.M., Evans, R., Brown, J., Feldman, G., and McClain, C. (1991). The Remote Sensing of Ocean Primary Productivity -- Use of a new Data Compilation to Test Satellite Algorithms. *J. of Geophys. Res.* Vol. 97 p. 2279-2293.

Chelton, D.B. and Schlax, M.G. (1991). Estimation of Time Averages from Irregularly Spaced Observations with Application to Coastal Zone Color Scanner Estimates of Chlorophyll Concentration. *J. of Geophys. Res.* Vol. 96 No. C8 p. 14,669-14,692.

Clark, D.K. (1981). Phytoplankton: algorithms for the Nimbus-7 CZCS, in *Oceanography from Space*, edited by J.R.F. Gower, p. 227-238, Plenum Press, New York.

Cullen, J.J. and Eppley, R.W. (1981). Chlorophyll maximum layers of the Southern California bight and possible mechanisms of their formation and maintenance. *Oceanol. Acta* 4, 1, p. 23-32.

Dickey, T.D. (1991). The emergence of Concurrent high resolution physical and his optical measurements in the upper ocean and their applications. *Reviews of Geophysics* 29, 3 p. 383-413.

Estep, L. Personal Communication.

Esaias, W., Feldman, G., McClain, C., and Elrod, J. (1986). Monthly satellite-derived phytoplankton pigment distribution for the North Atlantic. *EOS Trans* 67:44.

Feldman, G. (1989). Ocean Color. *EOS Tran.* 70:23 p. 634.

Feldman, G., Esaias, W.G., McClain, R.C., Evans, R., Brown, O. and Elrod, J. (1989). Ocean Color: Availability of the global data set. *EOS Tran.* AGU 70:23,643.

Firestone, J.K., Fu, G., Chen, J., Darzi, M. and McClain, C.R. (1989). PC Seapak: A state of the art image processing display and analyses system for NASA's Oceanographic research program. Proceedings of the Fifth Conference on *Interactive and Information Processing System for Meteorology, Oceanography and Hydrography*, Anaheim, Ca. Jan 29-Feb.3 American Meteorological Society.

Gordon, H.R. (1978). Removal of atmospheric effects from satellite imagery of the ocean. *Applied Optics* Vol. 17, p. 1631-1636.

Gordon, H.R. and Clark, D.K. (1980a). Atmospheric effects in remote sensing of phytoplankton pigments. *Boundary Layer Meteorology* Vol. 18, p. 299-313.

Gordon, H.R. and Clark, D.K. (1980b). Remote sensing optical properties of a stratified ocean: an improved interpretation. *Applied Optics* Vol. 19, p. 3428.

Gordon, H.R., and Clark, D.K. (1981). Clear water radiances for atmospheric correction of coastal zone color scanner imagery. *Applied Optics* Vol. 20, n. 24, p. 4175-4180.

Gordon, H.R. and McCluney, W.R. (1975). Estimation of the depth of sunlight penetration in the sea in remote sensing. *Applied Optics* Vol. 14, No. 2, p. 413-416.

Gordon, H.R., Clark, D.K., Brown, J.W., Brown, O.B., Evans, R.H. and Broenkow, W.W. (1983). Phytoplankton pigment concentration in the middle Atlantic bight; comparison of ship determination and CZCS estimates. *Applied Optics* Vol. 22,20.

Hovis, W.A., Clark, D.K., Anderson, F., Austin, R.W., Wilson, W.A., Butler, E.I., Ball, D., Gordon, H.R., Mueller, J.L., El-Sayed, S.F., Sturm, B., Wrigley, R.C., and Yentsch, C. (1980). Nimbus-7 coastal zone color scanner: system description and initial imagery. *Science* Vol. 210, (4465) p. 60-63.

Hughs Corporation (1987). System Concept for Wide-Field-of View Observations of Ocean Phenomena from Space. August NASA/EOSAT/HUGHES Report of the Joint EOSAT/NASA SeaWifs Working Group.

Kitchen, S.J., and Zaneveld, R. (1990). On the noncorrelation of the vertical structure of light scattering and chlorophyll in case I waters. *J. Geophys. Res.* Vol. 95 (C1).

Lewis, M.R., Kuring, N. and Yentsch, C.S. (1988). Global patterns of ocean transparency: Implications for new production of the open ocean. *J. of Geophys. Res.* Vol. 93 p. 6347-6856.

Lohrenz, S.E., Arnone, R.A., Wiesenburg, D.A. and DePalma, I.P. (1988). Satellite detection of transient enhanced primary production in the western Mediterranean Sea. *Nature* 335(6187) 245-247.

Martinez, R., Arnone, R.A. and Velasquez Z. (1990). Chlorophyll a and Respiratory Electron transport System Activity in Microplankton from the Surface Waters of the Western Mediterranean. *J. of Geophys. Res.* Vol. 95 No. C2 p. 1615-1622.

McClain, C.R., Fu, G., Darzi, M., and Firestone J. (1990). PC-Seapak User's Guide Version 3 NASA/GSFC 280 p.

Morel, A. and Prieur, L. (1977). Analysis of Variations in Ocean Color. *Limnology and Oceanog.* Vol. 22 No. 4 p. 709-722.

Morel, A. (1988) Optical modeling of the upper ocean in relation to its biogenous matter content (case 1 waters). *J. of Geophys. Res.* Vol. 93, No. C9 p. 10749-10768.

Mueller, J.L. (1984). Effects of Water Reflectance at 670 nm on Coastal Zone Color Scanner (CZCS) aerosol radiance estimates off the coast of Central California. *Ocean Optics VII, Monterey, Ca., Proc. of SPIE, Vol. 489 p. 170-186.*

Mueller, J.L., Trees, C.C., Arnone, R.A. (1990). Evaluation of Coastal Zone Color Scanner Diffuse attenuation coefficient algorithms for applications to coastal waters. *Ocean Optics X*, Vol. 1032, SPIE, Orlando Florida. p. 72-78.

Mueller, J.L. and Lange R.L. (1989). Bio-optical provinces of the Northeast Pacific Ocean: A provisional analysis. *Limnology and Oceanography*. 34(8) p. 1572-1586.

Platt, T.C., Caverhill, S., and Sathyendranath, S. (1991). Basin-Scale Estimates of Ocean primary production by remote sensing: The North Atlantic. *J. Geophys. Res.* Vol. 96 C8 p. 15147-15159.

Pressman, A.E., Holyer, R.J., Mueller, J.L., Harding, J.M., Martin, P., Arnone, R.A., and Curtis, J.E. (1989). Application of satellite ocean color imagery: plan and workshop report, Naval Oceanographic and Atmospheric Research Laboratory, SSC, MS, NOARL SP 080:321:89.

Smith, R.C. and Wilson, W.H. (1981). Ship and satellite bio-optical research in the California Bight. *Oceanography from Space* J.F.G. Gower ed., Plenum, New York, 281.

Terrie, G., Arnone, R.A. and Oriol, R.A. (1991). Modeling Global Surface Irradiance. *EOS* Vol. 72 No.17 April, p. 150.

Voss, K.J., Nolton, J.W., and Edwards, G.D. (1986). Ship shadow effects on apparent optical properties. In: M. Blizzard (ed.) *Ocean Optics VIII*, SPIE 637: 186-190.

Yoder, J.A., McClain, C.R. Blanton, J.O., and L.- Y. Oeg. (1987). Spatial sides in CZCS - chlorophyll imagery of the southeastern U.S. Continental Shelf. *Limnol Oceanogr.*, 32, 929-941.

Distribution List

Naval Research Laboratory
Stennis Space Center MS
39529-5004

ATTN: Code 104
Code 125L (6)
Code 125P
Code 211, G. Morris
Code 300
Code 311, K. Ferer
Code 320, J. McCaffrey
Code 321, A. Pressman
Code 322, L. Kantha,
P. Martin
Code 350, M. Harris

Oceanographer of the Navy
Chief of Naval Operations
U.S. Naval Observatory
34th & Massachusetts Ave. NW
Washington DC 20390-1800

ATTN: OP-096
CDR Malay
D. Montgomery
R. Winokur

Naval Oceanographic Office
Stennis Space Center MS
39522-5001

ATTN: E. Beason
B. Elenbis
K. Kirby
R. Lorens
K. Meyer
Library (2)
TD

NASA/GSFC
Greenbelt MD 20770
ATTN: Code 720, Dr. C. McClain

Office of Naval Research
800 N. Quincy Street
Arlington VA 22217-5000

ATTN: Code 112, E. Hartwig
M. Altalo, Biology
G. Gilbert
T. Kinder, Coastal Studies
R. Spinrad

Naval Command Control and
Ocean Surveillance Center
RDT&E Division
San Diego CA 92152-5000
ATTN: R. Buntzen

Head, Non-Acoustic Program
OP-21T2
1931 Jefferson Davis HWY.
Crystal Mall 3, Room C25
Arlington VA 22202
ATTN: Richard Lauer

Department of Oceanography
NPS Code OC/CU
Monterey CA 93943-5100
ATTN: D. Peter Clue

Jet Propulsion Laboratory
Pasadena CA 91109
ATTN: Dr. C. Davis

Department of Marine Science
UCLA
Los Angeles CA 90024
ATTN: Dr. T. Dickey

Lamont Doherty Geological
Laboratory
New York NY 10964
ATTN: Dr. J. Marra

University of Miami
RSMAS
Rickenacker Causeway
Miami FL 33124
ATTN: Dr. R. Evans

Department of Marine Sciences
University of South Florida
Tampa FL 33620
ATTN: Dr. K. Carder

Coastal Systems Station Dahlgren
Division
Naval Surface Warfare Center
Panama City FL 32407-5000
ATTN: N. Witherspoon
J. Loyd

San Diego State University
San Diego CA 92182
ATTN: Dr. J. Mueller

Department of Oceanography
TAMU
College Station TX 77843
ATTN: D. Wiesenburg

Minerals Management
1201 Elmwood Park Blvd.
New Orleans LA 70123
ATTN: Dr. Murry Brown

NMFS
Stennis Space Center MS 39527
ATTN: T. Leming

Goddard Space Flight Center
Wallops Island VA 23337
ATTN: Dr. F. Hoge

Department of Oceanography
University of Rhode Island RI
028812
ATTN: Dr. J. Yoder

Naval Research Laboratory
Washington DC 20375
ATTN: Library

REPORT DOCUMENTATION PAGE

Form Approved
OBM No. 0704-0188

Public reporting burden for this collection of information is estimated to average 1 hour per response, including the time for reviewing instructions, searching existing data sources, gathering and maintaining the data needed, and completing and reviewing the collection of information. Send comments regarding this burden or any other aspect of this collection of information, including suggestions for reducing this burden, to Washington Headquarters Services, Directorate for Information Operations and Reports, 1215 Jefferson Davis Highway, Suite 1204, Arlington, VA 22202-4302, and to the Office of Management and Budget, Paperwork Reduction Project (0704-0188), Washington, DC 20503.

1. Agency Use Only (Leave blank).		2. Report Date. May 1992	3. Report Type and Dates Covered. Final	
4. Title and Subtitle. Ocean Optical Database			5. Funding Numbers. Program Element No. 0603741N/ 0603785N Project No. P742/ 0120 Task No. Accession No. DN259069 Work Unit No. 13212W/93212R/ 9321CR	
6. Author(s). R.A. Arnone, R.A. Oriol*, G. Terrie, and L. Estep				
7. Performing Organization Name(s) and Address(es). Naval Oceanographic and Atmospheric Research Laboratory Ocean Science Directorate Stennis Space Center, MS 39529-5004			8. Performing Organization Report Number. NOARL Technical Note 254	
9. Sponsoring/Monitoring Agency Name(s) and Address(es). Naval Oceanographic and Atmospheric Research Laboratory Advanced Acoustics Program Office Stennis Space Center, MS 39529-5004 Naval Oceanographic and Atmospheric Research Laboratory ASW Oceanography Office Stennis Space Center, MS 39529-5004			10. Sponsoring/Monitoring Agency Report Number. NOARL Technical Note 254	
11. Supplementary Notes. *Planning Systems Incorporated Slidell, LA 70458				
12a. Distribution/Availability Statement. Approved for public release; distribution is unlimited.			12b. Distribution Code.	
13. Abstract (Maximum 200 words). The global ocean optical property of the diffuse attenuation coefficient at 490 nm $k(490)$, has been assembled into a database using satellite ocean color data from the Coastal Zone Color Scanner. The database representing 6 years of satellite coverage from 1978 to 1986 is at a spatial resolution of 20 km and is represented in monthly composites. The assemblage and format of the data are defined. Problems and limitations of using satellite ocean color for retrieving ocean $k(490)$ values are examined. The validation of the optical database from the satellite is accessed through comparison with in situ ship measurements of chlorophyll and diffuse attenuation coefficient.				
14. Subject Terms. Air Defense Initiative, Acoustic Modeling, Oceanography, Anti-Submarine Warfare			15. Number of Pages. 42	
			16. Price Code.	
17. Security Classification of Report. Unclassified	18. Security Classification of This Page. Unclassified	19. Security Classification of Abstract. Unclassified	20. Limitation of Abstract. SAR	